




Poly(U)-specific endoribonuclease ENDOU promotes translation of human *CHOP* mRNA by releasing uORF element-mediated inhibition

Hung-Chieh Lee^{1,†}, Chuan-Yang Fu^{1,†}, Cheng-Yung Lin¹, Jia-Rung Hu², Ting-Ying Huang², Kai-Yin Lo³, Hsin-Yue Tsai⁴, Jin-Chuan Sheu⁵ & Huai-Jen Tsai^{1,2,6,*} 

Abstract

Upstream open reading frames (uORFs) are known to negatively affect translation of the downstream ORF. The regulatory proteins involved in relieving this inhibition are however poorly characterized. In response to cellular stress, eIF2 α phosphorylation leads to an inhibition of global protein synthesis, while translation of specific factors such as CHOP is induced. We analyzed a 105-nt inhibitory uORF in the transcript of human *CHOP* (*huORF^{chop}*) and found that overexpression of the zebrafish or human ENDOU poly(U)-endoribonuclease (Endouc or ENDOU-1, respectively) increases *CHOP* mRNA translation also in the absence of stress. We also found that Endouc/ENDOU-1 binds and cleaves the *huORF^{chop}* transcript at position 80G-81U, which induces *CHOP* translation independently of phosphorylated eIF2 α . However, both ENDOU and phospho-eIF2 α are nonetheless required for maximal translation of *CHOP* mRNA. Increased levels of ENDOU shift a *huORF^{chop}* reporter as well as endogenous *CHOP* transcripts from the monosome to polysome fraction, indicating an increase in translation. Furthermore, we found that the uncapped truncated *huORF^{chop}*-69-105-nt transcript contains an internal ribosome entry site (IRES), facilitating translation of the cleaved transcript. Therefore, we propose a model where ENDOU-mediated transcript cleavage positively regulates *CHOP* translation resulting in increased CHOP protein levels upon stress. Specifically, *CHOP* transcript cleavage changes the configuration of *huORF^{chop}* thereby releasing its inhibition and allowing the stalled ribosomes to resume translation of the downstream ORF.

Keywords CHOP; human ENDOU-1; translational control; uORF; Zebrafish Endouc

Subject Category Translation & Protein Quality

DOI 10.15252/embj.2019104123 | Received 27 November 2019 | Revised 18 November 2020 | Accepted 30 November 2020 | Published online 28 January 2021

The EMBO Journal (2021) 40: e104123

Introduction

Almost half of human, mouse, and zebrafish mRNAs contain at least one upstream open reading frame (uORF) located at the 5' untranslated region (Iacono *et al*, 2005; Matsui *et al*, 2007; Calvo *et al*, 2009; Barbosa *et al*, 2013; Chew *et al*, 2013). While a few uORFs activate the downstream coding sequence (DCS) such as Cauliflower mosaic virus 35S RNA (Pooggin *et al*, 2001), most uORFs function as inhibitory elements to block DCS hereinafter termed as uORF-guided translational inhibition (uORF-TI) by different mechanisms (Kozak, 1987; Yaman *et al*, 2003; Vattem & Wek, 2004; Sachs & Geballe, 2006; Col *et al*, 2007; Zhou *et al*, 2008; Roberts *et al*, 2009; Chen *et al*, 2010; Palam *et al*, 2011). Such mechanisms include the nonsense-mediated decay pathway (He *et al*, 2003; Mendell *et al*, 2004; Sachs & Geballe, 2006; Ramani *et al*, 2009), the amino acid sequence of uORF-encoded peptide (von Arnim *et al*, 2014; Ebina *et al*, 2015), methylation of uORF2^{ATF4} (Zhou *et al*, 2018), stalled ribosome elongation at uORFs (Palam *et al*, 2011; Barbosa & Romão, 2014; Young *et al*, 2016; Young & Wek, 2016), and the stability of uORF secondary structure (Chew *et al*, 2016). Variable biological and structural properties of uORFs in each gene may affect the regulatory potential of uORFs (Barbosa *et al*, 2013). Consequently, only a limited number of uORFs have been functionally characterized such as the delayed translation reinitiation model for GCN4 and ATF4 (Young & Wek, 2016).

The mRNA encoding CCAAT/enhancer-binding protein homologous protein (CHOP) (Park *et al*, 1992; Barone *et al*, 1994) undergoes highly regulated translation through a single uORF element located at the 5'UTR of *CHOP*'s mRNA (Jousse *et al*, 2001). Previously, Chen *et al* (2010) proved that different stressors could induce a correspondingly different regulatory networks to control human uORF^{chop} (*huORF^{chop}*)-driven *CHOP* mRNA translation. Palam *et al* (2011) reported that phosphorylation of translation initiation factor eIF2 α at S51 facilitates ribosomal bypass of an inhibitory *huORF^{chop}*

1 Institute of Biomedical Sciences, Mackay Medical College, New Taipei City, Taiwan

2 Institute of Molecular and Cellular Biology, National Taiwan University, Taipei, Taiwan

3 Department of Agricultural Chemistry, National Taiwan University, Taipei, Taiwan

4 Institute of Molecular Medicine, School of Medicine, National Taiwan University, Taipei, Taiwan

5 Liver Disease Prevention and Treatment Research Foundation, Taipei, Taiwan

6 Department of Life Science, Fu Jen Catholic University, New Taipei, Taiwan

*Corresponding author. Tel: +886 2 326360303 #1724; E-mails: hjtsai@mmc.edu.tw, hjtsai@ntu.edu.tw

†These authors contributed equally to this work

to enhance *CHOP* mRNA translation. Young *et al* (2016) found that an RNA sequence encoding Ile-Phe-Ile (IFI) in *huORF^{chop}* is a key sequence for *CHOP* translation. However, while the inhibition of translation, as mediated by *huORF^{chop}*, has already been defined, it is still too early to conclusively declare that protein(s) other than canonical translation initiation factors might be directly involved in the translation of human *CHOP* mRNA during ER stress by suppressing its inhibitory uORF element.

Therefore, we aimed to address this question by using a zebrafish transgenic line, *huORFZ*, which harbors an inhibitory uORF of *huORF^{chop}* fused with GFP reporter serving as DCS and driven by cytomegalovirus promoter (Lee *et al*, 2011). The GFP signal is exclusively expressed in some specific subtype cells of the central nervous system within *huORFZ* embryos because they are highly responsive to heat-shock and hypoxic stresses (Lee *et al*, 2011; Zeng *et al*, 2016). The GFP reporter could be translated in these specific subtype cells because the inhibitory *huORF^{chop}* element was suppressed during stress. Therefore, we used laser microdissection to harvest GFP-expressing (+) and non-GFP-expressing (–) same subtype cells in the brain to identify *de novo* protein(s) that might play a repressive role in *huORF^{chop}*-TI and, hence, facilitate the translation of DCS. Microarrays and expression pattern analysis were used to select zebrafish Endouc, a human orthologue ENDOU (Lee *et al*, 2017), because it was significantly upregulated in the GFP(+) of brain during the applied stresses.

The eukaryotic ENDOU ribonuclease family consists of several enzymes that share amino acid homology with XendoU (Snijder *et al*, 2003; Renzi *et al*, 2006). This ENDOU family is broadly conserved from viruses to humans. For example, Nsp15, a viral orthologue of XendoU, plays an essential role in coronavirus replication (Bhardwaj *et al*, 2012) and host immune suppression (Ricagno *et al*, 2006). *Xenopus* XendoU is a uridylylate-specific, divalent cation-dependent enzyme that produces molecules with 2',3'-cyclic phosphate ends—this is a unique characteristic of this particular class of RNases involved in generating U16 and U86 small nucleolar RNAs through the cleavage of pre-mRNAs encoded within introns (Laneve *et al*, 2003; Gioia *et al*, 2005; Renzi *et al*, 2006). Human PP11 has been recently categorized as a member of the XendoU family. Despite its annotated function as a putative serine protease, PP11 is a placental-specific endoribonuclease. Moreover, the dysregulated expression of PP11 in tumor tissues may be associated with carcinogenesis (Inaba *et al*, 1982). Human ENDOU, or PP11, is a mammalian orthologue of zebrafish Endouc, and human ENDOU mRNA contains spliced variants encoding three different polypeptides, ENDOU-1 (NM_001172439.2), ENDOU-2 (NM_006025.4), and ENDOU-3 (NM_001172440.2) isoform (Lee *et al*, 2017).

Xenopus XendoU and human ENDOU play roles in cellular processes including the regulation of ER structure, RNA degradation, and cell survival (Poe *et al*, 2014; Schwarz & Blower., 2014). Moreover, *C. elegans* ENDOU-2 was reported to be involved in regulating cold intolerance and synaptic remodeling through caspase signaling suggesting that ENDOU may play a role in stress response (Ujisawa *et al*, 2018). However, it is unknown whether eukaryotic ENDOU family protein might also be involved in suppressing uORF-TI to facilitate the translation of *CHOP* mRNA.

In this study, we found that overexpression of zebrafish Endouc or human orthologue ENDOU isoform 1 (Endouc/ENDO-U1) could induce the translation of exogenous *huORF^{chop}*-tag reporter and

endogenous *CHOP* transcripts in HEK293T cells *in vitro* and zebrafish embryos *in vivo* without stress treatment, suggesting that Endouc/ENDO-U1 could suppress *huORF^{chop}*-TI. We also demonstrated that such blockade driven by Endouc/ENDO-U1 was dependent on its endoribonuclease activity. Endouc/ENDO-U1 could directly bind the *huORF^{chop}* transcript and cleave it at uridylylate-specific residue at 80G-81U. Moreover, increased Endouc resulted in a shift of *huORF^{chop}*-tagged and *CHOP* transcripts from monosomes toward polysomes. Furthermore, we demonstrated that the uncapped truncated *huORF^{chop}*-69-105-nt transcript possessed an internal ribosome entry site (IRES) activity. The increase of this IRES activity was dependent on the increase of Endouc/ENDO-U1. Therefore, we propose that Endouc/ENDO-U1 might facilitate the otherwise stalled ribosomes to suppress the inhibitory configuration caused by a *huORF^{chop}* cassette to result in the translation of the DCS of *CHOP* transcript during stress through its binding and ribonuclease activity on the *huORF^{chop}* transcript.

Results

Microarrays to screen for genes responsible for the translation of DCS during ER stress

To better understand the role of *huORF^{chop}*-TI *in vivo*, we first employed a zebrafish transgenic line *huORFZ* (Lee *et al*, 2011) which harbors *huORF^{chop}*-tagged reporter cDNA because GFP was exclusively apparent in stress-treated embryos. The number of GFP-expressing cells in the brain of *huORFZ* embryos at 72 h post-fertilization (hpf) was positively correlated with the duration of heat-shock treatment (Fig EV1A). Of the three different sections performed to isolate GFP(+) cells in the brain of stress-treated *huORFZ* embryos (Fig EV1B), more GFP(+) cells appeared on one slide from section 2 (Fig EV1C). Upon examining cells with immunostaining with the glial and neuronal markers to identify GFP(+) cells around tectal and telencephalic ventricles, we found that heat-shock-induced GFP(+) cells were a subtype of glial cells but not neurons (Fig EV1D).

Most importantly, we next studied the genes involved in *huORF^{chop}*-TI, and a microarray was performed to compare the expression levels of genes between GFP(+)- and GFP(–)-cells of the same subtype in the brain (Fig 1A). Based on Agilent *GeneSpring* software analysis, a total of 643 under-represented transcripts and 1,014 over-represented transcripts were identified in GFP(+) cells from heat-shock stress when compared to GFP(–) cells. A total of 1,346 under-represented transcripts and 2,210 over-represented transcripts were identified in GFP(+) cells from hypoxic stress versus GFP(–) cells. Moreover, a total of 298 over-represented transcripts and 104 under-represented transcripts were identified for both stresses (Fig 1B and Appendix Table S1).

Screening used the three steps: First, we focused on the highly upregulated genes from the microarray data. Typically, we would use an antisense morpholino-knockdown strategy to determine highly downregulated putative genes. However, it was easier to confirm whether putative genes were involved in *huORF^{chop}*-TI simply through microinjection of mRNAs in non-stressed zebrafish embryos. In total, 298 highly upregulated genes were picked for cloning. Of these, 183 candidate genes were successfully amplified

by PCR and cloned into the pGEMTeasy vector for whole-mount *in situ* hybridization (WISH) riboprobe synthesis; 107 out of the 183 candidates were successfully cloned into the pCS2 vector for *in vitro* mRNA synthesis. Each of these prepared mRNAs was then individually microinjected into zebrafish *huORFZ* embryos. Strikingly, most injected embryos were either lethal or devoid of GFP expression before 24 hpf with the notable exception of those introduced with mRNAs of endonuclease polyU-specific C (*endouc*), eukaryotic

translation initiation factor 3 subunit Hb (*eif3hb*), transcription elongation factor A (SII) (*teca2*), and peroxiredoxin 6 (*prbx6*). When these four putative genes were overexpressed in untreated *huORFZ* embryos, we observed that GFP reporter was detectable in all embryos (Appendix Fig S1A). Among these four candidates, only embryos injected with *endouc* mRNA could induce the GFP reporter specifically at the CNS tissues; the injection of *ela3l* mRNA (false positive control) did not (Fig 1E).

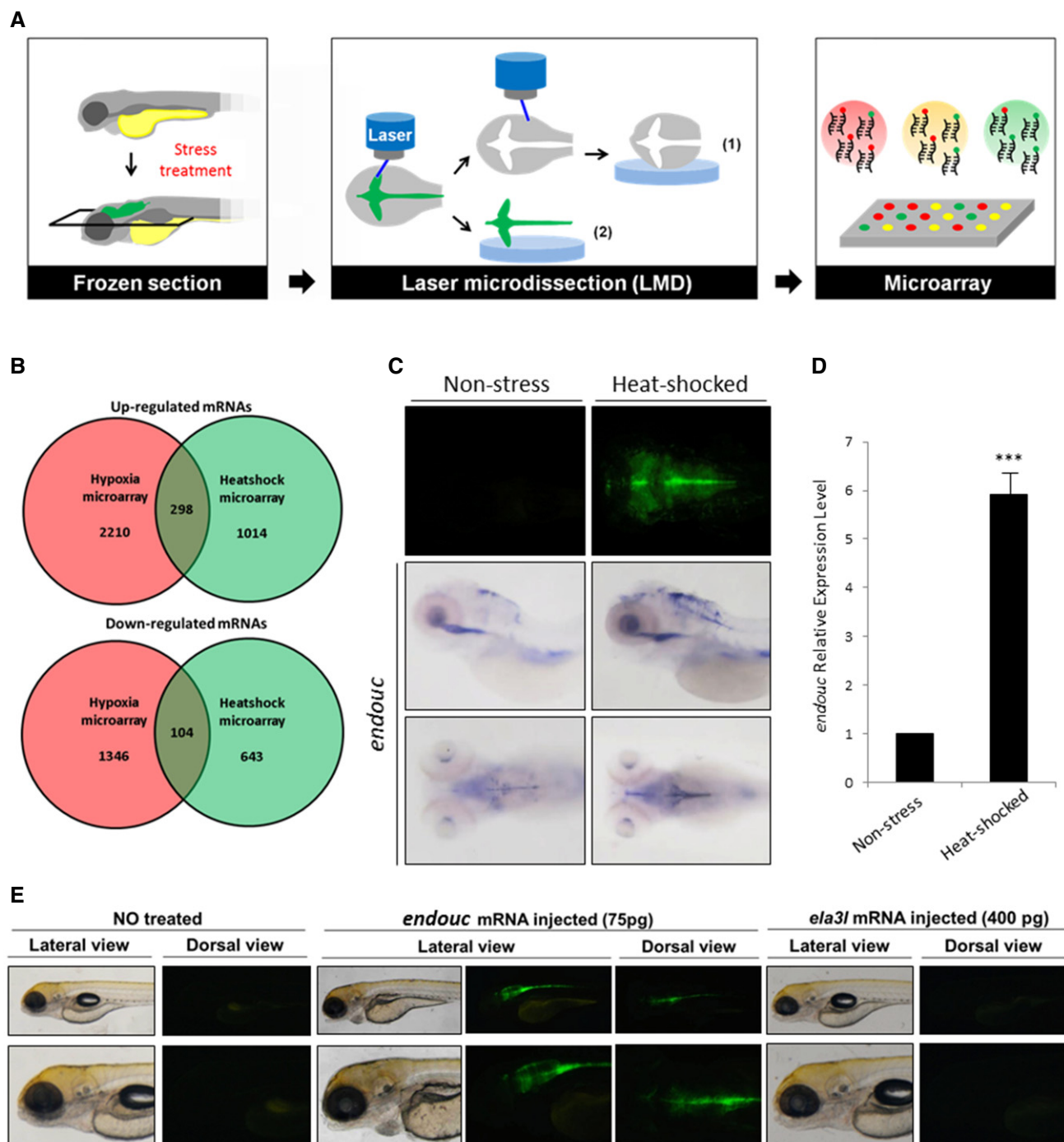


Figure 1.

Figure 1. Method of searching for candidate genes identified as potentially involved in translational control mediated by *huORF^{chop}* transcript through their upregulation in GFP-expressing cells.

- A Schematic diagram illustrating the separation of GFP-expressing and non-GFP-expressing cells from stress-treated zebrafish embryos of transgenic line *huORFZ* using LMD methods followed by microarrays.
- B Graphical representation of two microarray expression analyses. A total of 298 over-represented transcripts and 104 under-represented transcripts were obtained from both microarrays.
- C Upper panels: top view of EGFP expressed in zebrafish embryos derived from zebrafish transgenic line *huORFZ* under non-stress and heat-shock treatment. Middle panels: lateral view of *endouc* expression patterns in embryos under non-stress condition and treated with heat-shock. Lower panels: top view of *endouc* expression patterns.
- D Quantitative RT-PCR determined the relative expression level of *endouc* mRNA in non-stress- and heat-shock-treated embryos. Values representing the non-stress- and heat-shocked conditions were calculated from three independent experiments and presented as mean \pm SD ($n = 3$). Student's *t*-test was used to determine significant differences between each group ($***P < 0.001$).
- E The *endouc* and *ela3l* (negative control) mRNAs were separately microinjected into zebrafish embryos from *huORFZ* at one-cell stage. Upper panels: observation of GFP signal expressed in *huORFZ* embryos at 72 hpf. Lower panels: magnification of pictures corresponding to the upper panels.

Second, we performed WISH to examine whether these putative genes were upregulated in embryos after stress treatment. This step resulted in the discovery of two genes involved in translation including *EIF3HB* and *TCEA2* as well as two genes that encoded enzymes including *endouc* and heme oxygenase 1a (*hmox1*); these had a significant upregulation in heat-shock-treated embryos compared to non-stress control embryos (Appendix Fig S1B). We also found that some candidate genes were unchanged or slightly increased in the heat-shock-treated embryos compared to non-stress control embryos such as chymotrypsinogen B1 (*ctrb1*), elastase 3 like (*ela3l*), serine protease 35 (*prss35*), death-associated protein 1b (*dap1b*), peroxiredoxin 6 (*prdx6*), and glutamate-cysteine ligase (*gclc*) (Appendix Fig S1C). We noticed that *endouc* transcript was significantly upregulated in brain compared to the control untreated embryos (Fig 1C). This upregulated expression pattern of *endouc* in the brain corresponded to the results of the GFP reporter, which was also significantly expressed in the brain of *huORFZ* embryos treated with heat-shock (Fig 1C). The level of *endouc* transcript was markedly increased around the tectal ventricle and upper hindbrain after embryos were treated with heat-shock stress (Fig 1C).

Therefore, based on our stepwise elimination approach to determine the genes involved in *huORF^{chop}*-TI, zebrafish *endouc* (accession number *si:dkey-103i16.2*)—which is conserved to the human orthologue ENDOU gene (Lee et al, 2017)—became the primary hit for further study for two reasons. First, the *endouc* transcript displayed a 5.39- and 2.85-fold increase of expression in the heat-shocked-treated and hypoxia-treated GFP(+) cells, respectively (Appendix Table S1). Second, real-time qPCR result of *endouc* transcript was consistent with those obtained from the microarray data and WISH (Fig 1C and D). Therefore, we propose that Endouc might be a novel non-ribosomal protein able to suppress *huORF^{chop}*-TI control thus facilitating the translation of DCS during ER stress.

Transfection of Endouc/ENDOU-1 alone is sufficient to drive the translation of DCS reporter even in the absence of stress

We quantified the increase of downstream luciferase (luc) reporter induced by overexpression of Endouc through *in vivo* study. Wild-type (WT) zebrafish embryos were microinjected with a plasmid carrying *huORF^{chop}-luc*, a dual-luc-control vector (pHRG-TK), and an Endouc-Flag-overexpression vector. Under normal conditions, the zebrafish embryos injected with all three plasmids noted above exhibited 5.3-fold higher luc activity than that of the control group,

which was injected with plasmids puORF^{chop}-luc, pCS2 vector, and pHRG-TK (Fig 2A). The elevated luc activity that occurred in the Endouc-injected embryos under normal conditions was consistent with that of the Endouc-injected embryos under stress conditions such as the application of heat-shock (Fig 2A).

We next performed an *in vitro* study, in which the above plasmids were transfected into HEK293T cells. Under normal conditions, luc activity was increased ~2.6-fold when the vector containing Endouc was transfected (Fig 2B). This was consistent with the results of Endouc-overexpressed cells under stress conditions such as treatment with thapsigargin (TH)—an ER stress inducer (Fig 2B). The consistency of both *in vitro* and *in vivo* results led us to conclude that the overexpression of Endouc causes a dramatic increase in the DCS reporter expression suggesting that Endouc facilitates the translation of *huORF^{chop}*-tag transcript.

To investigate whether overexpression of Endouc can increase CHOP translation, we overexpressed Endouc at the one-cell stage of zebrafish embryos treated with heat-shock at 72 hpf. We then analyzed CHOP level at 96 hpf. The results demonstrated that overexpression of Endouc in zebrafish embryos increased the protein level of CHOP both in non-stress and heat-shock conditions (Fig 2C). Similar results were observed in the *in vitro* study where overexpression of Endouc in HEK293T and HeLa cells increased CHOP expression (Fig 2D and E).

The translation of CHOP is tightly linked to the degree of p-eIF2 α during stress (Palam et al, 2011), and we asked if overexpression of Endouc would correlate with increased levels of p-eIF2 α . Western blot results showed that overexpression of Endouc in zebrafish embryos, as well as HEK293T and HeLa cells, did increase the level of p-eIF2 α (Fig 2C–E) suggesting that Endouc overexpression induces an increase of p-eIF2 α . These data demonstrated that Endouc functions as a positive regulator of CHOP translation during stress response.

Like zebrafish Endouc, the human orthologue ENDOU-1 can suppress the inhibitory *huORF^{chop}* element

Transfection of any one of three plasmids containing the three isoforms of human ENDOU could greatly induce the translation of reporter gene resulting in increased luc activity up to ~4.8-fold, which is higher than that achieved by the transfection of zebrafish *endouc* expression plasmid (Fig EV2A and B). Similar to TH-treated cells, transfection of overexpressed human ENDOU-1 in cells could

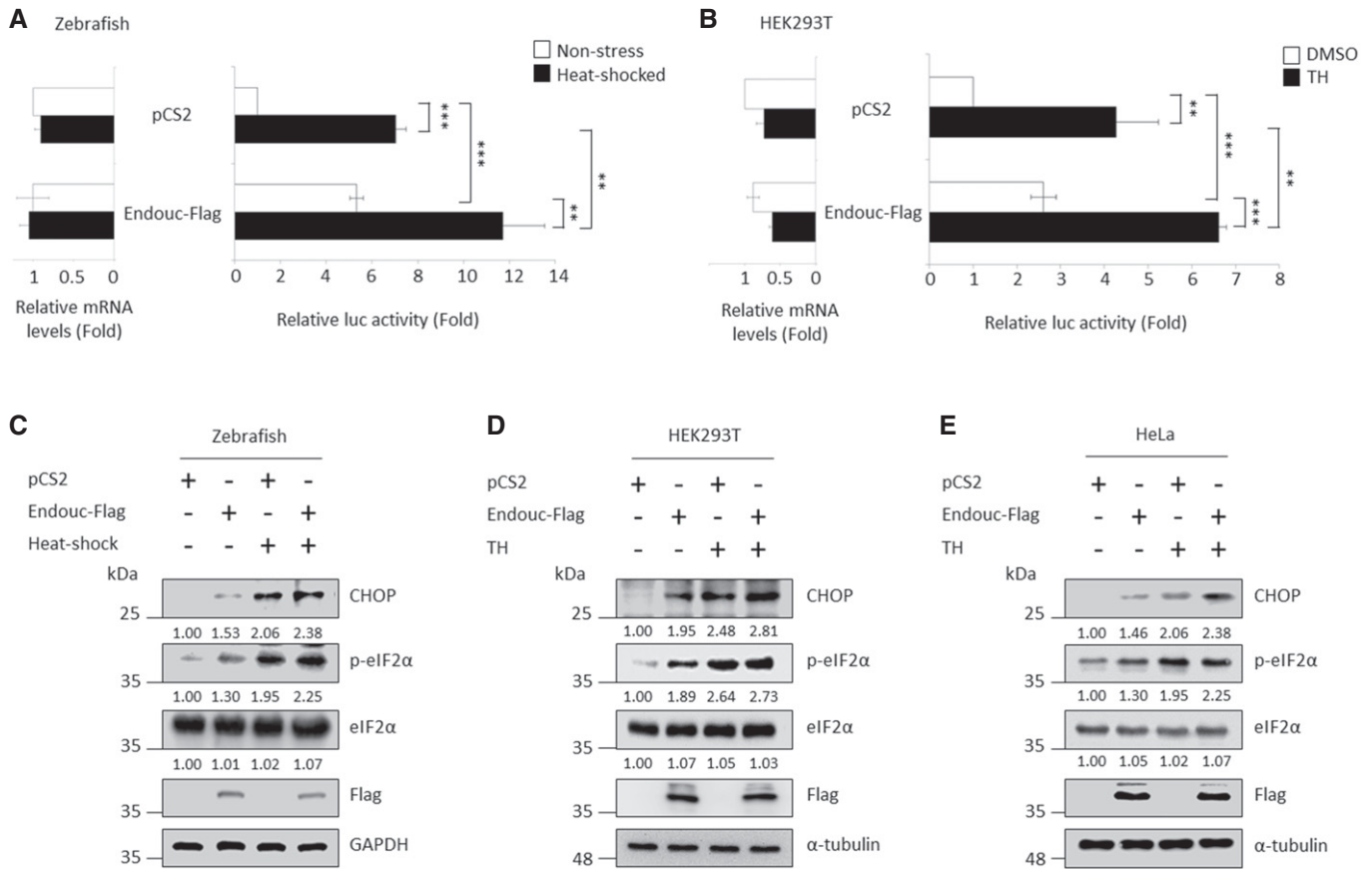


Figure 2. Overexpression of zebrafish Endouc blocks *huORF^{chop}-TI* and translates downstream reporter gene in the absence of stress.

- A** Histograms show the luc activity obtained from zebrafish embryos microinjected simultaneously with puORF^{chop}-luc, pHRG-TK, and each indicated plasmid followed by analysis of luc activity at 96 hpf. Embryos microinjected with pCS2 vector during normal condition (non-stress; blank column) served as a control group, while the microinjected embryos treated with 40°C at 72 hpf for 1 h were the heat-shocked group (solid column). The relative luc activity of microinjected embryos shown on the right was normalized by the amount of RNA in the injected embryos shown on the left. The relative luc activity was represented by the fold increase of Fluc/Rluc ratio over that obtained from the control group (this was normalized to 1). The luc activity mediated by the *huORF^{chop}* transcript was measured by dual-luciferase assay, and its corresponding *huORF^{chop}-luc* transcript was measured by RT-qPCR. Values representing the non-stress and stress condition were calculated from three independent experiments and presented as mean \pm SD ($n = 3$). Student's *t*-test was used to determine significant differences between each group (** $P < 0.005$, *** $P < 0.001$).
- B** Histograms present the luc activity obtained from HEK293T cells co-transfected with puORF^{chop}-luc, pHRG-TK, and each indicated plasmid and then treated with either DMSO (control group) or thapsigargin (TH; stress group), followed by analysis of luc activity. Cells transfected with pCS2-vector and kept at normal condition served as a control group. The relative luc activity of transfected cells shown on the right was normalized by the amount of mRNA in the transfected cells shown on the left. The relative luc activity was represented by the fold increase of Fluc/Rluc ratio over that obtained from pCS2-transfected control group (this was normalized to 1). The luc activity mediated by the *huORF^{chop}* transcript was measured by dual-luciferase assay, and its corresponding *huORF^{chop}-luc* transcript was measured by RT-qPCR. Values representing the non-stress and stress conditions were calculated from three independent experiments and presented as mean \pm SD ($n = 3$). Student's *t*-test was used to determine significant differences between each group (** $P < 0.005$, *** $P < 0.001$).
- C–E** Western blot analysis of proteins, as indicated, in (C) zebrafish embryos, (D) HEK293T cells and (E) HeLa cells. GAPDH and α -tubulin served as internal controls. Protein levels relative to each internal control are presented below each lane.

Source data are available online for this figure.

effectively suppress the repressive effect mediated by *huORF^{chop}* transcript, in turn, enhancing the translation of the reporter gene (Fig EV2A).

To further confirm the suppressive effect of ENDOU-1 on *huORF^{chop}-TI*, we studied the time course expression of endogenous ENDOU-1 in HEK293T cells treated with stress. As shown in Fig EV2C, a rapid increase in the expression of ENDOU-1 was observed 1 h after stress treatment, reaching a high level after 2 h; this level was maintained for up to 8 h. CHOP, however, exhibited a slow response and reduced expression after 8 h. The p-eIF2 α protein

showed early expression, but it then slowed after 4 h. Therefore, we suggest that human ENDOU-1 is also a stress-responsive gene with a suppressive effect on *huORF^{chop}-TI*.

Endoribonuclease activity of Endouc/ENDO-1 is required to suppress the inhibitory *huORF^{chop}* structure

We next sought to mechanistically explain the involvement of zebrafish Endouc in *huORF^{chop}-TI*. To accomplish this, a series of Endouc deletion constructs (Fig 3A) were co-transfected with

puORF^{chop}-luc. A luc activity assay was then performed to analyze the effects of these constructs on regulating *huORF^{chop}*-TI both *in vivo* (zebrafish embryos) and *in vitro* (HEK293T cells).

Compared with control, the luc activity was greatly increased in recipients with intact Endouc, Endouc^{Δ1–25}, Endouc^{Δ26–136}, and Endouc^{Δ299–310}; it was slightly reduced in recipients with Endouc^{Δ137–298} (Fig 3B and C; Appendix Fig S2A and B). We noticed that transfection of Endouc^{Δ137–298} failed to suppress *huORF^{chop}*-mediated mRNA translation in recipients under both normal and stress conditions (Fig 3B). Western blot analysis also demonstrated that the protein levels of p-eIF2 α and CHOP were greatly reduced in cells expressing Endouc^{Δ137–298} both *in vivo* and *in vitro* (Fig 3D and E) suggesting that the key domain of Endouc for regulating *huORF^{chop}*-TI is located at residues 137–298. E243, H244, E249, H259, and K302 are necessary for human ENDOU-2 endoribonuclease activity (Laneve *et al*, 2008), while H162 and K224 are necessary for *Xenopus* XendoU RNase activity (Schwarz & Blower, 2014). Interestingly, the key residues required to suppress *huORF^{chop}*-TI of Endouc are all within the 137–298 residues. On the basis of this evidence, we mutated zebrafish Endouc at H181 (Endouc^{H181A}) and K242 (Endouc^{K242A}) to alanine to generate two endoribonuclease-deficient Endouc proteins (Fig 4A). Cells and embryos transfected with intact Endouc showed evidence of a *huORF^{chop}*-TI blockage. However, no luc activity was induced when embryos were transfected with both Endouc^{H181A} and Endouc^{K242A} (Fig 4B and C; Appendix Fig S2C and D). Furthermore, Western blot analysis demonstrated that overexpression of intact Endouc in recipients increased the protein levels of p-eIF2 α and CHOP at normal condition, while overexpression of both Endouc^{H181A} and Endouc^{K242A}, for which endoribonuclease activity was lost in recipients, did not (Fig 4D and E). These results were consistent with both TH-treated cells and heat-shock-treated embryos. Therefore, we conclude that the endoribonuclease activity of zebrafish Endouc is critical to blocking *huORF^{chop}*-TI.

Next, we demonstrated that overexpression of ENDOU-1 increased the expression levels of p-eIF2 α and CHOP in HEK293T and U373MG cells (Fig EV3A and B). However, when we mutated residue H285 of ENDOU-1 (responsible for endoribonuclease activity), we found that overexpression of the ENDOU-1^{H285A} mutant affected neither p-eIF2 α nor CHOP levels (Fig EV3A and B) suggesting that the increase of p-eIF2 α and CHOP levels induced by ENDOU-1 is dependent on the endoribonuclease activity of ENDOU-1. We further confirmed that both Endouc/ENDOU-1 were functionally conserved increasing p-eIF2 α and CHOP expression and playing a suppressive role in *huORF^{chop}*-TI through their endoribonuclease activity. The GFP(+)-expressing cells were zebrafish glial-like cells, while the U373MG cells were human glioblastoma–astrocytoma cells. Therefore, these results also strengthened our hypothesis that Endouc/ENDOU-1 plays important roles in *CHOP* translation in glial-like cells of zebrafish embryos.

Increased CHOP protein level by overexpression of Endouc is specific but independent of ER stress

To further prove the specific roles of Endouc/ENDOU-1 in facilitating *CHOP* mRNA translation, we first determined if CHOP induced by Endouc/ENDOU-1 resulted from ER stress caused by Endouc/ENDOU-1 overexpression. We examined the mRNA level of spliced

xbp1 and protein level of ER stress markers in Endouc/ENDOU-1-expressing cells. Compared to TH-treated cells, Endouc/ENDOU-1-overexpressed cells only displayed increased GADD34, p-eIF2 α , and CHOP, while spliced *xbp1* mRNA and other stress factors were not increased (Fig EV4A, B and D). GADD34 was induced in Endouc- and ENDOU-1-overexpressing cells (Fig EV4D), which could have resulted from the increase of p-eIF2 α induced by overexpression of Endouc/ENDOU-1 as supported by Novoa *et al* (2003) who reported that eIF2 α phosphorylation promotes GADD34 expression. Most stress markers were unaffected suggesting the specific induction of p-eIF2 α and CHOP expression by Endouc/ENDOU-1 again confirming that Endouc/ENDOU-1 was functionally conserved as described above. Specifically, Endouc/ENDOU-1 could increase eIF2 α phosphorylation and suppress *huORF^{chop}*-mediated repression of mRNA translation to increase CHOP expression through their endoribonuclease activities.

The RT-quantitative PCR (RT-qPCR) data indicate that the *CHOP* mRNA level did not increase in cells overexpressing Endouc/ENDOU-1. Rather, *CHOP* mRNA was slightly reduced in these cells (Fig EV4C). In contrast, the amount of CHOP protein was increased in cells overexpressing Endouc/ENDOU-1. Collectively, these data proved that Endouc/ENDOU-1 positively regulates *CHOP* expression at the translational level.

Endouc/ENDOU-1 induces CHOP translation

To investigate the effect of Endouc/ENDOU-1 expression and eIF2 α phosphorylation on *CHOP* translation, we first employed HEK293T cells treated with ISRIB—an integrated stress response inhibitor that can reverse the effect of eIF2 α phosphorylation thereby inhibiting eIF2 function. HEK293T cells were transfected with an expression vector containing either vector only or *endouc* cDNA for 24 h; this was then treated with either DMSO or 200 nM ISRIB followed by an analysis of the level of CHOP protein. Similar to the CHOP protein weakly present in the control, CHOP was only slightly detected in ISRIB-treated cells in the absence of Endouc (lanes 1 and 2 of Fig 5A). However, CHOP was significantly detected in the Endouc-expressing cells in the absence of ISRIB (lane 3 of Fig 5B). Interestingly, we found that the protein level of CHOP expressed in cells treated with Endouc plus ISRIB was lower than that in cells treated with Endouc plus p-eIF2 α (lanes 3 versus 4 in Fig 5B) suggesting that both Endouc/ENDOU-1 expression and eIF2 α phosphorylation impact CHOP translation.

Next, we studied the control mechanism between Endouc and p-eIF2 α on suppressing *huORF^{chop}*-TI under stress. HEK293T cells were transfected with vector containing Endouc and Endouc^{K242A} mutant, and then treated with TH and/or 200 nM ISRIB followed by an analysis of the protein level of CHOP. Compared to cells treated with TH, the CHOP protein was reduced in cells treated with TH plus ISRIB (lanes 2 versus 3 in Fig 5B) suggesting that ISRIB treatment could reduce the CHOP level induced by TH. This result was consistent with that obtained in Endouc-expressing cells (lanes 4 versus 5 in Fig 5B). The level of CHOP expressed in cells treated with Endouc/TH/ISRIB was higher than that of cells treated with vector/TH/ISRIB (lanes 3 versus 5 in Fig 5B). CHOP was reduced in the Endouc^{K242A} mutant (lanes 4 versus 6 in Fig 5B) compared to Endouc-expressing cells. When Endouc-expressing cells and Endouc^{K242A}-expressing cells were treated with TH and ISRIB, CHOP

was significantly reduced in the Endouc^{K242A}-expressing cells in comparison to the Endouc-expressing cells (lanes 5 versus 7 in Fig 5B). Unlike the expression profile of CHOP protein, we noticed that p-eIF2 α was always reduced in ISRIB-treated cells. This suggests that Endouc alone is sufficient to induce *CHOP* translation independent of the effect of eIF2 α phosphorylation.

Our next step was to strengthen the hypothesis that Endouc alone is sufficient to induce *CHOP* translation and does so independent of eIF2 α phosphorylation. To accomplish this, we employed mouse embryonic fibroblast (MEF) WT and mutant S51A cells that cannot phosphorylate eIF2 α due to an S51A knock-in mutation at the eIF2 α phosphorylation site (Scheuner *et al*, 2001). First, when MEF WT cells were treated with TH, both p-eIF2 α and ENDOU-1

were induced compared to DMSO-treated control cells (Fig 5C) indicating that Endouc/ENDO-1 induced by stress is conserved among fish, mice, and humans. Additionally, the pronounced upregulation of Endouc/ENDO-1 failed to materialize in MEF S51A mutant cells treated with TH (Fig 5C) suggesting that p-eIF2 α also facilitates Endouc/ENDO-1 upregulation and that increased p-eIF2 α is required for the full expression of Endouc/ENDO-1 to facilitate *CHOP* translation during ER stress.

Second, we further confirmed if Endouc/ENDO-1 could induce *CHOP* translation in the absence of p-eIF2 α . To address this question, MEF WT and S51A mutant cells were individually transfected with a plasmid harboring cDNA encoded with either Flag-tagged Endouc/ENDO-1 or Endouc/ENDO-1^{K242A/H285A} mutant followed

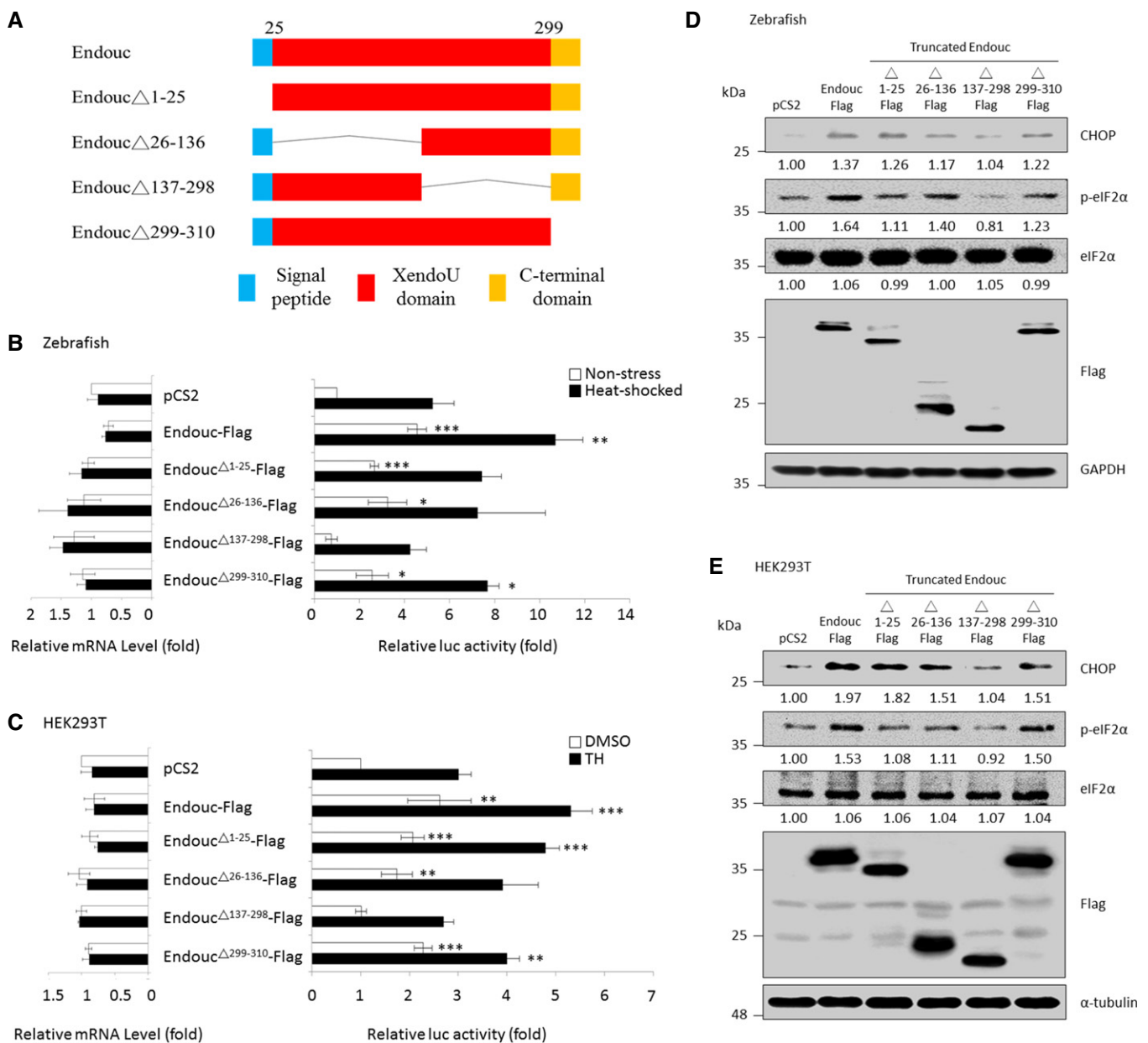


Figure 3.

Figure 3. Identification of Endouc functional domain involved in regulating *huORF^{chop}*-TL.

- A Schematic representation of zebrafish Endouc protein and its internal deletion mutants.[‡]
- B Histograms presenting the relative luc activity obtained from zebrafish embryos microinjected simultaneously with puORF^{chop}-luc, pHRG-TK, and each of the expression plasmids as indicated followed by analysis of luc activity at 96 hpf. Embryos microinjected with pCS2 vector during normal condition served as a control group (non-stress; blank column), while the microinjected embryos treated with 40°C at 72 hpf for 1 h were the heat-shocked group (solid column). The relative luc activity of microinjected embryos shown on the right was normalized by the amount of RNA in the injected embryos shown on the left. The relative luc activity is represented by the fold increase in Fluc/Rluc ratio over that obtained from control group. The luc activity mediated by the *huORF^{chop}* element was measured by a dual-luciferase assay, and its corresponding *huORF^{chop}*-luc transcript was measured by RT-qPCR.
- C Histograms presented the luc activity obtained from HEK293T cells co-transfected with puORF^{chop}-luc, pHRG-TK, and each one of the plasmids as indicated and treated with either DMSO (control group) or thapsigargin (TH; stress group) followed by analysis of luc activity. The luc activity of cells transfected with pCS2 vector and kept at normal condition served as a control group. The relative luc activity of transfected cells shown on the right was normalized by the amount of RNA in the transfected cells shown on the left. The relative luc activity is represented by the fold increase of Fluc/Rluc ratio over that obtained from pCS2-transfected control group normalized as 1. The luc activity mediated by the *huORF^{chop}* transcript was measured by the dual-luciferase assay, and its corresponding *huORF^{chop}*-luc transcript was measured by RT-qPCR.
- D Zebrafish embryos at one-cell stage were microinjected with plasmids as indicated, followed by extraction of embryonic proteins at the 96-hpf stage. Protein levels of CHOP, p-eIF2 α , total eIF2 α , Endouc-Flag, and its variants were detected using Western blot analysis. GAPDH served as an internal control.
- E HEK293T cells were transfected with indicated plasmids followed by analysis of the protein levels of CHOP, p-eIF2 α , total eIF2 α , Endouc-Flag, and its variants using Western blot. The α -tubulin served as an internal control. Protein levels relative to each internal control are presented in each lane.

Source data are available online for this figure.

by analysis of the protein level of CHOP and p-eIF2 α . In MEF WT cells, the results showed that both CHOP and p-eIF2 α were significantly induced in Endouc/ENDOU-1-overexpressing cells compared to untreated control cells, while neither CHOP nor p-eIF2 α was induced by Endouc/ENDOU-1^{K242A/H285A} mutant (Fig 5D and E). Nevertheless, CHOP was still increased in MEF S51A mutant cells treated with TH, although the level of CHOP was decreased in S51A mutant cells compared to WT cells (Fig 5D and E), suggesting that Endouc/ENDOU-1 could induce *CHOP* translation in the absence of p-eIF2 α through its endoribonuclease activity because the endoribonuclease-deficient mutant Endouc/ENDOU-1^{K242A/H285A} could not induce *CHOP* translation. We also noticed that GADD34 could be induced by Endouc/ENDOU-1 in MEF WT cells but not in MEF S51A mutant cells (Fig 5D and E), suggesting that GADD34 is not directly induced by Endouc/ENDOU-1. Rather, the GADD34 induced by Endouc/ENDOU-1 is dependent on p-eIF2 α .

CHOP was increased in the TH-treated MEF S51A mutant cells, and thus, we conclude that (i) endoribonuclease activity of Endouc/ENDOU-1 is necessary for Endouc/ENDOU-1 to induce CHOP and p-eIF2 α expressions; (ii) *CHOP* translation induced by Endouc/ENDOU-1 during stress is independent of eIF2 α phosphorylation unlike the p-eIF2 α -dependent induction of GADD34; and (iii) CHOP reached a maximal level in the presence of both Endouc/ENDOU-1 and p-eIF2 α during ER stress.

Finally, we performed siRNA to knock down ENDOU-1 in HEK293T cells. Versus cells transfected with siCTRL-siRNA after incubation with TH, the CHOP in HEK293T cells transfected with ENDOU-1-siRNA was reduced significantly in both the absence and presence of TH (Fig 5F). We conclude that overexpression of Endouc/ENDOU-1 results in an increase in the p-eIF2 α and CHOP levels—this is specific and independent of ER stress. Nevertheless, both Endouc and p-eIF2 α are required for *CHOP* mRNA translation to reach a maximal level.

Endouc/ENDOU-1 induces eIF2 α phosphorylation through the PKR pathway

The coronaviral EndoU family protein Nsp15 has been associated with PKR activity in host cells (Kindler et al, 2017). Since Endouc and ENDOU-1 are members of the EndoU family of proteins, we

next studied a possible role of RNA-activated protein kinase PKR in the induction of eIF2 α phosphorylation and translational upregulation of *CHOP* as a result of ENDOU-1 expression. We analyzed the p-PKR level in Endouc/ENDOU-1-expressing cells and found that the p-PKR level was induced significantly in HEK293T, HeLa, and MEF WT cells treated with TH compared to DMSO-treated control cells (Fig 6A; Appendix Fig S3A and B). Moreover, the p-PKR level was induced in Endouc/ENDOU-1-overexpressing cells without stress treatment. Meanwhile, the endoribonuclease-deficient Endouc^{K242A}/ENDOU-1^{H285A}-overexpressing cells did not induce p-PKR suggesting that Endouc/ENDOU-1 induces PKR phosphorylation through its endoribonuclease activity.

We further employed PKRA6, which is a PKR dominant-negative mutant that lacks six amino acids in its catalytic domain and, thus, fails to phosphorylate eIF2 α (Koromilas et al, 1992; Romano et al, 1995; Tu et al, 2012). The level of p-eIF2 α was reduced when Endouc/ENDOU-1 and PKRA6 were co-expressed in cells (Fig 6B; Appendix Fig S3C and D). Compared to the control cells, even though p-eIF2 α was absent in cells co-transfected with Endouc/ENDOU-1 and PKRA6, CHOP protein was still present (Fig 6B; Appendix Fig S3C and D), albeit in minimally detectable level suggesting that inhibition of PKR pathway in Endouc-expressing cells only blocks the induction of p-eIF2 α . Moreover, the cells transfected with mutant Endouc^{K242A}/ENDOU-1^{H285A} failed to induce PKR, eIF2 α phosphorylation, and CHOP protein (Fig 6B; Appendix Fig S3C and D). This line of evidence suggests that Endouc/ENDOU-1 induces eIF2 α phosphorylation through the PKR pathway.

Taken together, it can be concluded that (i) the increase of eIF2 α phosphorylation induced by Endouc is dependent on PKR phosphorylation; (ii) Endouc/ENDOU-1 induces the PKR-eIF2 α pathway through its endoribonuclease activity; and (iii) expression between Endouc/ENDOU-1 and p-eIF2 α exhibits feedback loop control.

Small RNA fragments cleaved from *huORF^{chop}* transcript under stress were detected in *in vivo* and *in vitro* systems

Northern blot analysis was performed to further study whether the *huORF^{chop}* transcript could be cleaved *in vivo* and *in vitro* under stress. An increase in small RNA fragments was observed in

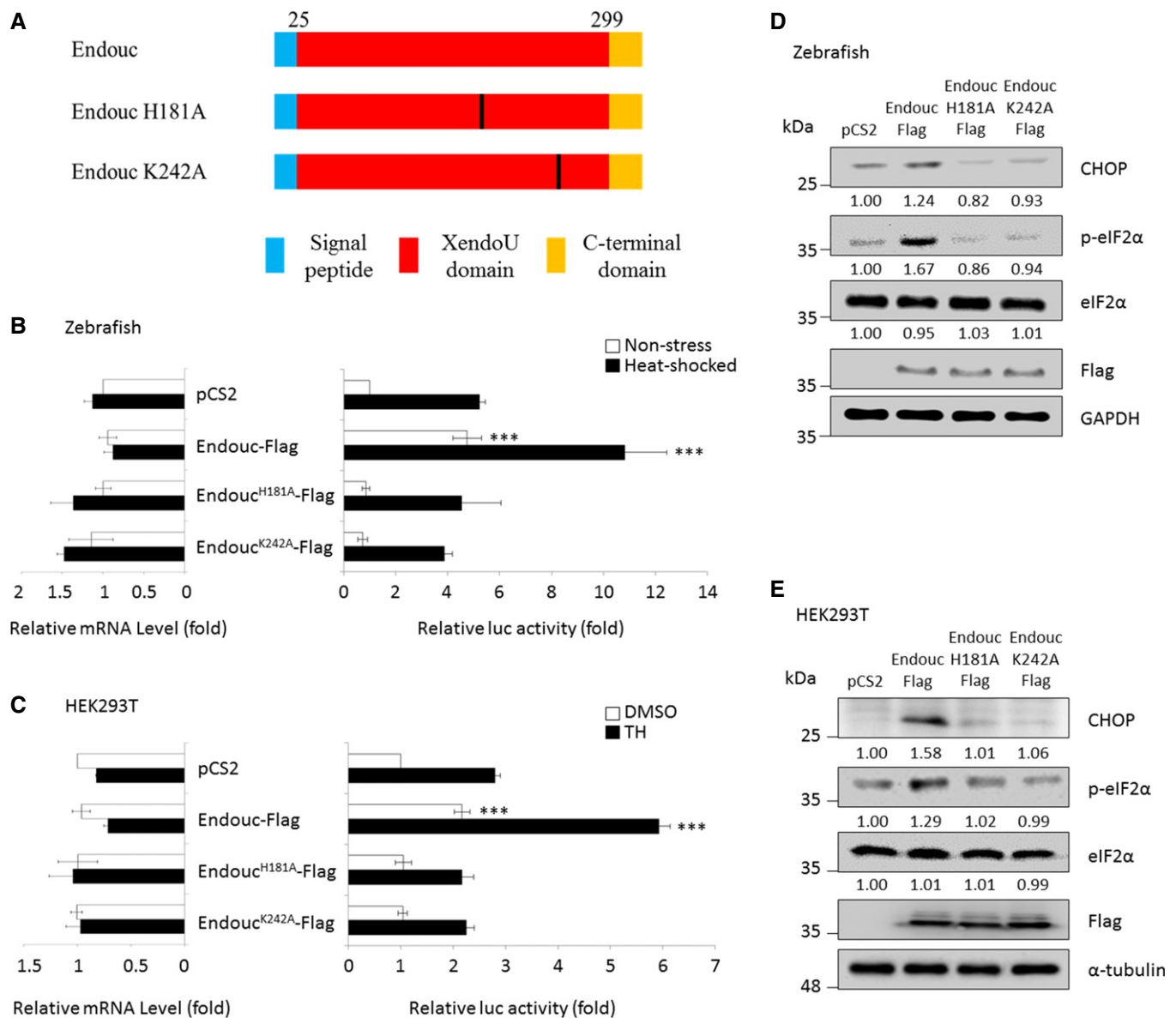


Figure 4. The positive effect of Endouc on p-eIF2 α and CHOP expressions is dependent on its endoribonuclease activity.

A Schematic representation of zebrafish Endouc protein and its internal deletion mutants.[‡]

B Histograms presented the relative luc activity obtained from zebrafish embryos microinjected simultaneously with puORF^{chop}-luc, phRG-TK, and each one of the expression plasmids as indicated followed by analysis of luc activity at 96 hpf. Embryos microinjected with pCS2 vector during normal condition (non-stress; blank column) served as a control group, while the microinjected embryos treated with 40°C at 72 hpf for 1 h were the heat-shocked group (solid column). The relative luc activity of microinjected embryos shown on the right was normalized by the amount of RNA in the injected embryos shown on the left. The relative luc activity was represented by the fold increase of Fluc/RIuc ratio over that obtained from control group. The luc activity mediated by the *huORF^{chop}* transcript was measured by dual-luciferase assay, and its corresponding *huORF^{chop}*-luc transcript was measured by RT-qPCR.

C Histograms presented the luc activity obtained from HEK293T cells co-transfected with puORF^{chop}-luc, phRG-TK, and each one of the plasmids as indicated; these were treated with either DMSO (control group) or thapsigargin (TH; stress group) followed by analysis of luc activity. The luc activity of cells transfected with pCS2 vector and kept at normal condition served as a control group. The relative luc activity of transfected cells shown on the right was normalized by the amount of RNA in the transfected cells shown on the left. The relative luc activity was represented by the fold increase of Fluc/RIuc ratio over that obtained from pCS2-transfected control group normalized as 1. The luc activity mediated by the *huORF^{chop}* transcript was measured by the dual-luciferase assay, and its corresponding *huORF^{chop}*-luc transcript was measured by RT-qPCR.

D Zebrafish embryos at one-cell stage were microinjected with plasmids as indicated followed by extraction of embryonic proteins at the 96-hpf stage. Protein levels of CHOP, p-eIF2 α , total eIF2 α , Endouc-Flag, and its variants were detected using Western blot analysis. GAPDH served as an internal control.

E HEK293T cells were transfected with indicated plasmids followed by analysis of the protein levels of CHOP, p-eIF2 α , total eIF2 α , Endouc-Flag, and its variants using Western blot. Here, α -tubulin served as an internal control. Protein levels relative to each internal control were presented in each lane.

Source data are available online for this figure.

[‡]Correction added on June 1 2021, after first online publication: "Single" was corrected to "Signal" in Figs 3A and 4A.

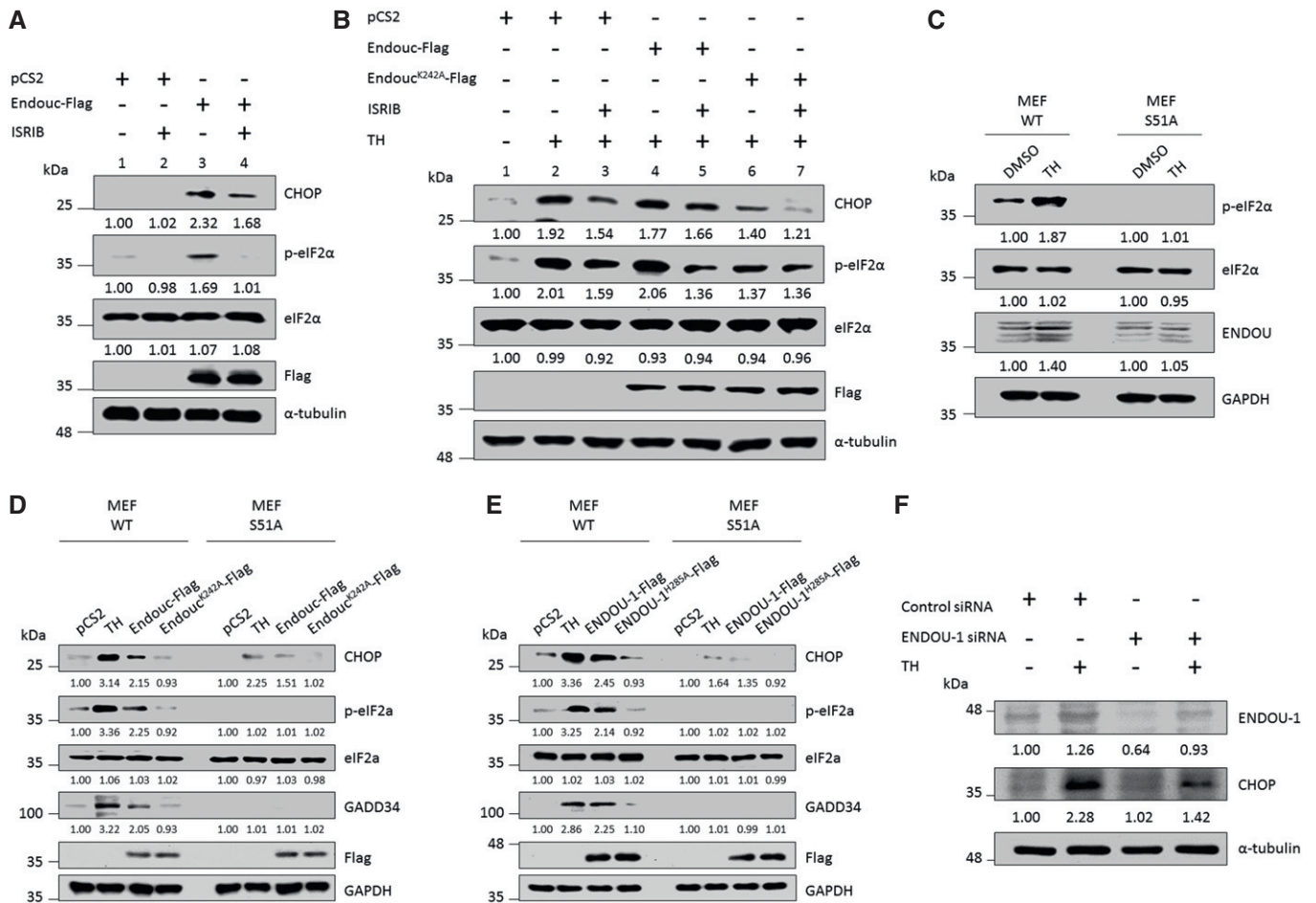


Figure 5. Besides p-eIF2α, Endouc/ENDOU-1 is another key protein that causes an increase in the CHOP protein level.

A HEK293T cells were transfected with plasmids as indicated for 24 h and treated with DMSO or 200 nM ISRIB for 2 h followed by analysis of the protein level of CHOP, p-eIF2α, total eIF2α, and Endou-Flag using Western blot. The α-tubulin served as an internal control. Protein levels relative to each internal control are presented in each lane.

B HEK293T cells were transfected with plasmids as indicated for 24 h and treated with DMSO, thapsigargin (TH), ISRIB, or TH plus ISRIB for 2 h followed by analysis of the protein level of CHOP, p-eIF2α, total eIF2α, Endou-Flag, and its variants using Western blot. The α-tubulin served as an internal control. Protein levels relative to each internal control were presented at each lane.

C MEF wild-type (WT) and its eIF2α^{S51A} mutant (S51A) cells were treated with 1 μg of TH for 4 h followed by Western blot analysis of p-eIF2α, total eIF2α, and ENDOU. GAPDH served as an internal control. Protein levels relative to each internal control are presented in each lane.

D, E MEF WT and mutant S51A cells were transfected with plasmids as indicated for 24 h and treated with either DMSO or TH for 4 h followed by analysis of the protein levels of CHOP, p-eIF2α, total eIF2α, GADD34, Endou-Flag and ENDOU-1-Flag using Western blot. GAPDH served as an internal control. Protein levels relative to each internal control were presented at each lane.

F HEK293T cells were transfected with negative control siRNA and ENDOU-siRNA for 48 h. After treatment, protein lysates were prepared and subjected to Western blot analysis for ENDOU-1 and CHOP detection using antibodies. The α-tubulin served as an internal control. Protein levels relative to each internal control were presented in each lane.

Source data are available online for this figure.

heat-shock-treated *huORFZ* embryos (Fig 7A), suggesting that the *huORF^{chop}-gfp* transcript could be cleaved *in vivo* under stress. In HEK293T cells, compared to DMSO-treated control cells, endogenous *CHOP* mRNAs were increased, but small mRNAs of fewer than 50 nucleotides (nts) were significantly increased in TH-treated cells. Meanwhile, the internal control *gapdh* mRNA did not change in either DMSO-treated or TH-treated cells (Fig 7B) suggesting that *huORF^{chop}* transcripts could be cleaved under stress.

Endouc/ENDOU-1 cleaves *huORF^{chop}* RNA at uridylylates within a specific structure

It was reported that human ENDOU-1 could cut at uridylylates of oligonucleotide GGAACGUAUCCUUUGGGAG derived from small nucleolar RNAs containing multiple natural cleavage sites for XendoU (Laneve *et al*, 2003, 2008). Interestingly, this XendoU-specific cutting sequence corresponds to sequences ranging from 72 to 91 nts of *huORF^{chop}* transcript. When we used the Rochester Predict

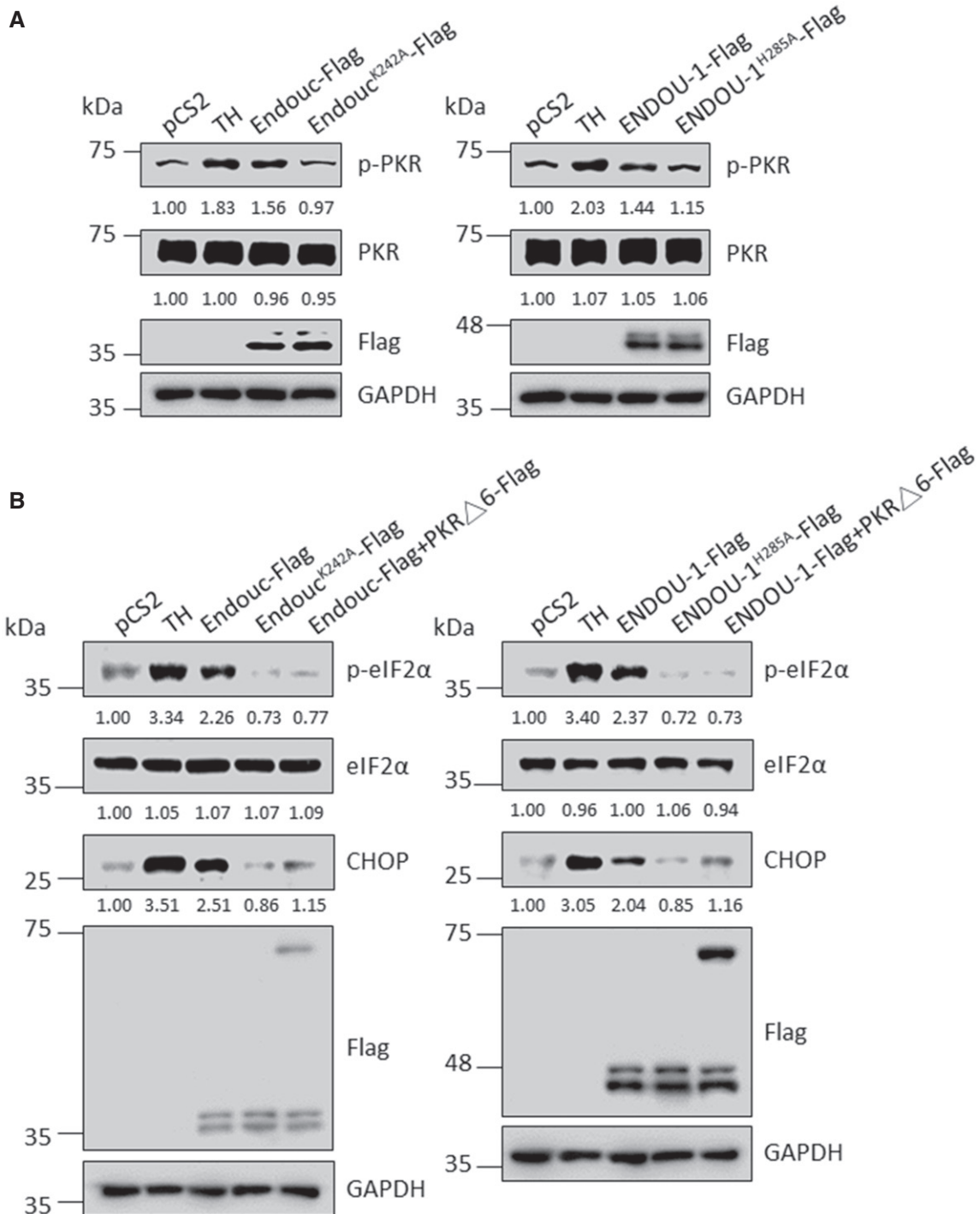


Figure 6. Endouc/ENDOU-1 induces the phosphorylation of eIF2 α through the PKR pathway.

A MEF wild-type (WT) cells were transfected with plasmids as indicated for 24 h and treated with either DMSO or thapsigargin (TH) for 4 h followed by analysis of the protein level of p-PKR, total PKR, Endouc-Flag and ENDOU-1-Flag. GAPDH served as an internal control. Protein levels relative to each internal control were presented at each lane.

B MEF WT cells were transfected with plasmids as indicated for 24 h and treated with either DMSO or TH for 4 h followed by analysis of the protein levels of p-eIF2 α , total eIF2 α , CHOP, Endouc-Flag and ENDOU-1-Flag. GAPDH served as an internal control. Protein levels relative to each internal control were presented at each lane. The results obtained from the two trials are shown on the left and right.

Source data are available online for this figure.

secondary structure server, we found that the sequences from 72 to 91 nts of *huORF^{chop}* transcript *per se* could plausibly form a stem-loop structure similar to that described by Laneve *et al* (2008) (Fig 7C), and that it could be repeatedly presented if the full-length sequence of *huORF^{chop}* transcript were used to predict its secondary structure (Appendix Fig S4).

ENDO has a ribonuclease domain that can cleave RNAs at UU dinucleotides or a single U *in vitro* (Caffarelli *et al*, 1997; Laneve *et al*, 2003, 2008; Bhardwaj *et al*, 2006). Therefore, we performed an RNase activity assay to examine whether zebrafish Endouc could cleave *huORF^{chop}* transcript. Three fragments were generated in a dose-dependent manner when biotin was labeled at the 3'-end of *huORF^{chop}* transcript (Fig 7D). However, cleaved fragments could not be detected when uridylates were mutated to guanines within 69–92 nt of *huORF^{chop}* transcript (Fig 7D). Competition experiments also showed that the WT *huORF^{chop}* transcript, but not mutant RNA, could reduce the cleavage signal (Fig 7E). Furthermore, mutant Endouc^{K242A} failed to digest *huORF^{chop}* transcript (Fig 7D). This line of evidence suggests that the cleavage of Endouc on *huORF^{chop}* transcript is specific to uridylates and that the amino acid residue at K242 is required for RNase activity of Endouc.

Endouc binds directly with *huORF^{chop}* transcript

To confirm binding between Endouc and *huORF^{chop}* transcript, we performed RNA EMSA using biotin-labeled, full-length *huORF^{chop}* transcript and Endouc. Compared to luc mRNA (Appendix Fig S5A), the results confirmed that Endouc could bind specifically with the *huORF^{chop}* transcript in a dose-dependent manner (Fig 7F). However, the band shift shown on the EMSA gel was abolished by the increase of unlabeled *huORF^{chop}* transcript (Appendix Fig S5B). Moreover, Endouc bound neither luc mRNA nor *huORF^{chop}* DNA (Fig 7F), suggesting that the binding between *huORF^{chop}* transcript and Endouc is specific.

RNA EMSA demonstrated that Endouc could still bind with the mutated *huORF^{chop}* transcript (Appendix Fig S5C) although binding efficiency was relatively weak relative to the normal *huORF^{chop}* transcript. However, Endouc failed to cleave mutated *huORF^{chop}* transcript (Fig 7E) in which uridylates within 72–91 nts were mutated. Thus, it is clear that binding in the presence of uridylylate is permissive for the specific cleavage of *huORF^{chop}* transcript by Endouc.

Endouc facilitates stalled ribosomes to suppress the inhibitory *huORF^{chop}* element and plays a positive role in the translation of *CHOP* mRNA

We next performed polysome profiling to directly examine the role of Endouc in regulating *huORF^{chop}*-TI. HEK293T cells were transiently transfected with Endouc- or Endouc^{K242A}-expression vector and treated with cycloheximide to arrest elongating ribosomes on mRNAs. Their lysates were then subjected to sucrose gradient ultracentrifugation, and sample fraction were pooled into three groups shown in Figure 8A: free ribosomal subunits (Fractions 1 and 2), monosomes (Fractions 3–6), and light and heavy polysomes (Fractions 7–12). Compared to control cells, overexpression of Endouc caused an inhibition of global translational initiation as documented by the loss of heavy polysomes; overexpression of Endouc^{K242A} did not change the polysome profile (Fig 8A). Western blot analysis

demonstrated that both Endouc and Endouc^{K242A} were mostly found in the monosome and light polysome fractions, whereas a small percentage of Endouc was found in the heavy polysome fractions (Fig 8A). Although no difference was observed in the distribution at each polysome fraction between protein levels of Endouc and Endouc^{K242A}, the overexpression of Endouc could reduce global translation, while overexpression of Endouc^{K242A} did not change the polysome profile. Moreover, LC-MS/MS analysis proved that the major proteins interacting with recombinant Endouc-Flag were ribosomal proteins and proteins involved in translation (Appendix Table S2). This evidence suggested that blockade of *huORF^{chop}*-TI via Endouc is dependent on its endoribonuclease activity.

We next measured the levels of endogenous *CHOP* and exogenous *huORF^{chop}*-tagged luc transcripts among the sucrose fractions. In the control cells, the *huORF^{chop}*-tagged luc (Fig 8B) and *CHOP* mRNAs (Fig 8C) were largely associated with monosomes (Fractions 4 and 5). However, in Endouc-overexpressing cells, the *huORF^{chop}*-tagged luc and *CHOP* mRNAs displayed a shift of 43 and 37% of transcripts from monosome toward light polysomes (Fractions 6–8), respectively. In contrast, similar to the control group, overexpression of endoribonuclease-deficient mutant Endouc^{K242A} did not trigger these mRNAs into the light polysome fraction (Fractions 6–8). The addition of Endouc caused a higher percentage of luc reporter and *CHOP* mRNAs to shift from the monosome toward the light polysome fraction to proceed with continuous translation (Appendix Fig S6A and B).

The RNA fragment cleaved by Endouc at the 80G-81U of *huORF^{chop}* transcript is found in polysome fractions

Next, to isolate and characterize *CHOP* mRNA after nuclease activity, we performed an experiment in which exogenous *huORF^{chop}*-luc mRNA and endogenous *huORF^{chop}*-*CHOP* mRNA were isolated from polysome fractions and characterized them after nuclease activity. After the sequences of these isolated mRNAs were confirmed using 5'RACE, we focused on finding truncated sequences derived from the *huORF^{chop}* transcript in the polysome fractions isolated from both exogenous *huORF^{chop}*-luc mRNA and endogenous *huORF^{chop}*-*CHOP* mRNA groups. Specifically, the first nucleotide of major truncated mRNAs was the T at the nucleotide position of 81 (81T) (Fig 8D and E) suggesting the following: First, exogenous *huORF^{chop}*-luc (42%, *n* = 14) and endogenous *huORF^{chop}*-*CHOP* mRNAs (55%, *n* = 11) were cleaved by Endouc, a uridylylate-specific endoribonuclease, at the nucleotide position between 80G and 81U (80G-81U). Second, the non-5'-capped truncated forms of exogenous *huORF^{chop}*-luc transcript and endogenous *huORF^{chop}*-*CHOP* mRNA were undergoing translation.

Interestingly, the identified Endouc cleavage site at 80G-81U was located at the hairpin structure of *huORF^{chop}* cassette, which is one of the predicted sites recognized and cleaved by Endouc (Fig 7C). Moreover, 80G-81U sequences were located next to the Ile-Phe-Ile sequence (82A-90A nts), which is an essential sequence that allows the *huORF^{chop}* motif to act as an inhibitory element to repress the translation of *CHOP* mRNA at normal state (Young *et al*, 2016). Therefore, we demonstrated cleavage of both exogenous *huORF^{chop}*-luc and endogenous *huORF^{chop}*-*CHOP* transcripts by Endouc at 80G-81U.

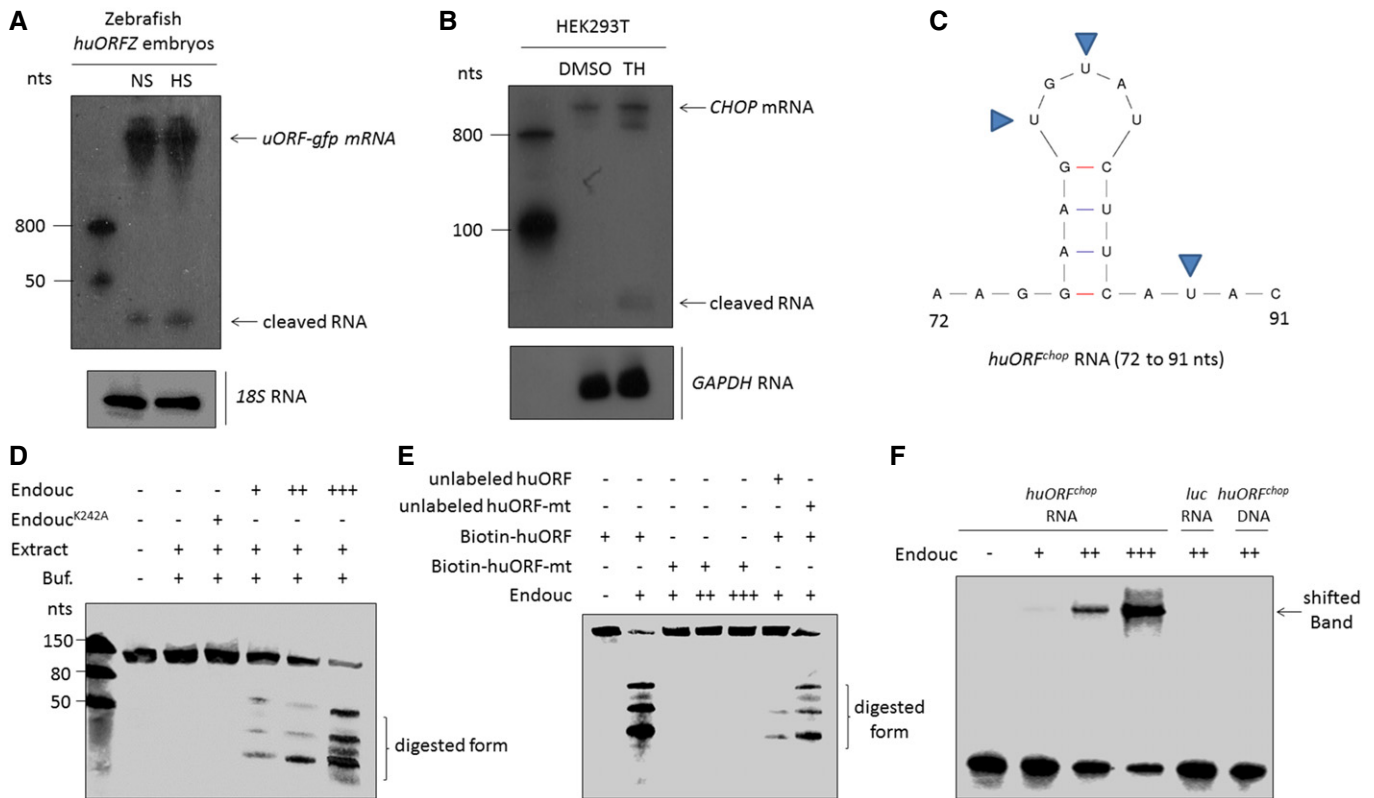


Figure 7. Endouc can bind and cleave the *huORF^{chop}* transcript.

- A Northern blot analysis to detect the endogenous *huORF^{chop}*-tagged *gfp* (*uORF-gfp*) mRNA and its cleaved form in zebrafish embryos of transgenic line *huORFZ* treated with non-stress condition (NS) or heat-shocked (HS) stress. Zebrafish 18S rRNA served as an internal control. The RNA fragments cleaved from *huORF^{chop}* transcript were detected.
- B Northern blot analysis to detect endogenous *CHOP* mRNA in HEK293T cells treated with either DMSO (control group) or thapsigargin (TH). Human *GAPDH* RNA served as internal control. The RNA fragments cleaved from *CHOP* mRNA were detected.
- C The predicted RNA sequences of Endouc recognition site on *huORF^{chop}* transcript from 72 to 91 nts are illustrated. The predicted cleavage sites at uridylates (U) are indicated by arrowheads.
- D, E The cleavage activity of Endouc was studied using materials presented at each lane. Endouc^{K242A}: Endouc mutant; Extract: incubated in cell extracts; and Buf: reaction buffer. RNA probe without adding reaction buffer served as a negative control. The predicted cleavage sites (U) were mutated to generate mutant *huORF^{chop}* transcript (unlabeled huORF-mt) and labeled by biotin (biotin-huORF-mt). Unlabeled competitor RNA was added in reactions at five times higher than that of the biotinylated probe.
- F Electrophoretic mobility shifted assay of RNA. Biotin-labeled *huORF^{chop}* transcript was reacted with the increased amount of Endouc. The positions of free RNA (free probe) and RNA-protein complex (shifted band) were indicated on the right. The *luc* 105-nt RNA and single-stranded *huORF^{chop}* 105-nt DNA served as negative controls.

The uncapped truncated transcript derived from *huORF^{chop}* RNA did not decay immediately in cells

To determine whether overexpression of Endouc could change the turnover of *CHOP* mRNA, we treated Endouc-overexpressing MEF cells with TH followed by actinomycin D treatment. The half-life of *CHOP* transcript from the control (no stress treatment) and TH-treated cells was 2.61 and 2.4 h, respectively (Fig EV5A and B). This is consistent with the previous study reported by Rutkowski *et al* (2006) and Young *et al* (2016) who demonstrated that the half-life of *CHOP* transcript is 2–3 h, while overexpression of Endouc reduced the half-life of *CHOP* transcript to 2.18 h suggesting that overexpression of Endouc did not significantly impact the turnover of *CHOP* transcript.

We next determined whether this uncapped truncated transcript would decay immediately or remain in cells. To accomplish this, MEF cells were transfected with pCS2-Endouc-Flag followed by

actinomycin D treatment; an adaptor at the 5' end was added for cDNA synthesis. We then used primers that could specifically target the adaptor-linked cleavage of *huORF^{chop}* cDNA for our qPCR experiment (see Materials and Methods). Compared to the half-life between capped full-length *huORF^{chop}* and uncapped truncated *huORF^{chop}* transcripts, we found that the half-life of full-length *huORF^{chop}* transcript was 3 h, while the half-life of uncapped truncated *huORF^{chop}* transcript was reduced to about 43 min (Fig EV5C), suggesting that the uncapped truncated *huORF^{chop}* transcript could remain in cells for up to 90 min. Since some translated mRNAs have a half-life shorter than 1 h (Sharova, *et al*, 2009) or even shorter than 30 min (Raghavan *et al*, 2002), the half-life of *huORF^{chop}* 81–105-nt transcript is reasonably sufficient for *CHOP* translation. We also demonstrated that more *CHOP* transcript correlated with more *CHOP* protein further suggesting that the truncated transcripts cleaved from *huORF^{chop}* may contribute to the translation of *CHOP* protein (Fig EV5D).

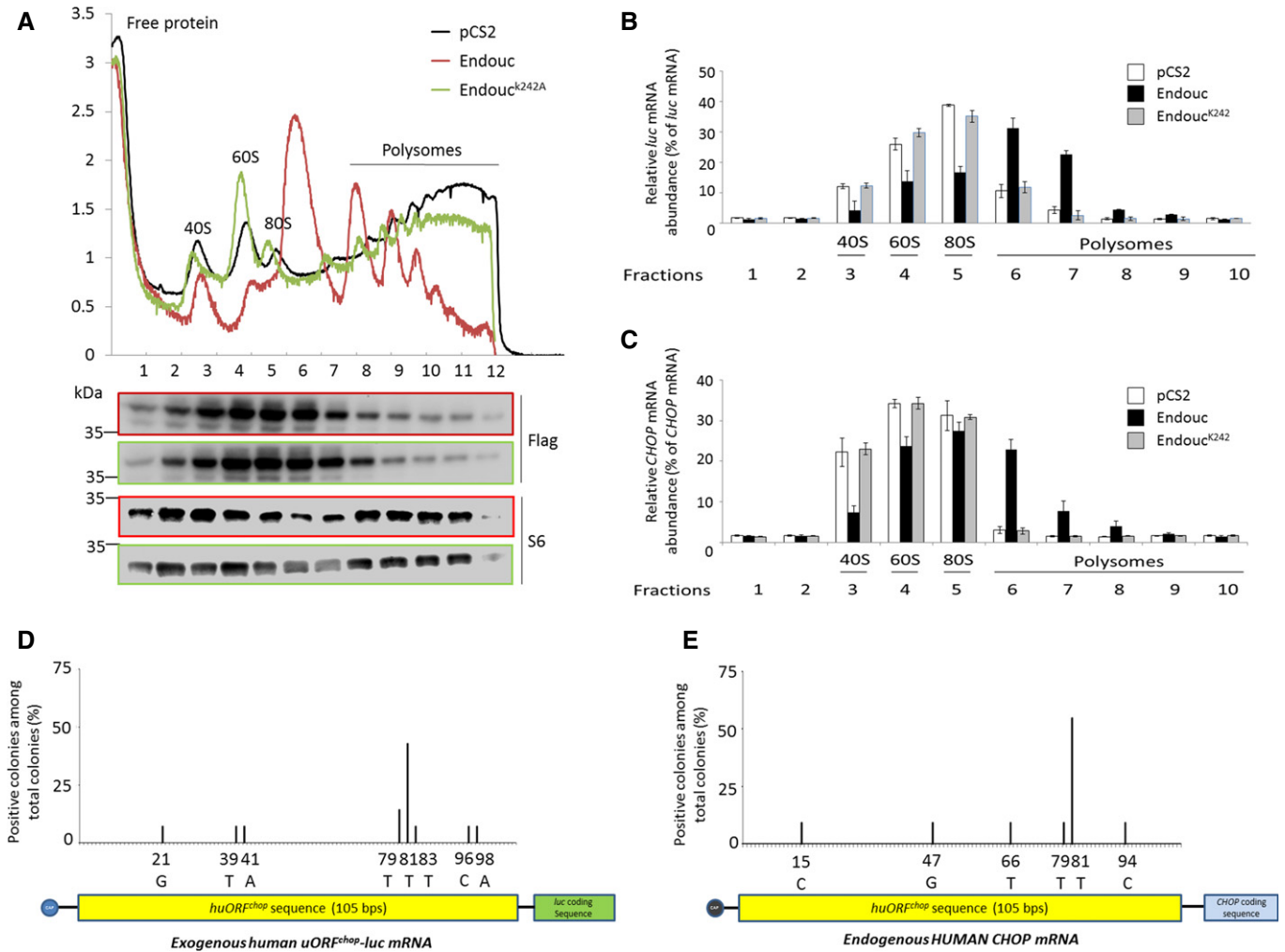


Figure 8. Endouc associates with monosomes and plays a key role in regulating *CHOP* post-translation.

A HEK293T cells were transfected with pCS2 vector (black), pCS2-Endouc (red), and pCS2-Endouc^{K242A} (green) for 24 h and subjected to either DMSO (control) or thapsigargin (TH; stress) treatment for 1 h. The lysates of transfected cells were applied to polysome profile analysis (PPA). The sucrose gradient from top to bottom was shown from left to right, respectively. The sedimentation of 40S, 60S, 80S, and polysomes was indicated. Lysates from control, Endouc-expressing, and Endouc^{K242A}-expressing cells were applied to PPA. The resulting fractions were TCA-precipitated, analyzed by SDS-PAGE, and subjected to Western blot using antibodies against Flag and S6. Upper and lower rows of Flag- and S6 blots were Endouc- and Endouc^{K242A}-expressing cells, respectively.

B, C The lysates from control (pCS2), Endouc-expressing (Endouc), and Endouc^{K242A}-expressing (Endouc^{K242A}) cells were applied to PPA. The resulting fractions from 1-10 collected from sucrose gradient were subsequently subjected to RT-qPCR assay to quantify (B) exogenous *huORF^{chop}-luc* mRNA and (C) endogenous *CHOP* transcripts (*CHOP* mRNA). The distribution of relative abundance of *luc* and *CHOP* transcripts contained in each fraction was determined.

D, E HEK293T cells were co-transfected with pCS2-Endouc and *huORF^{chop}-luc* for 24 h and then subjected to DMSO or TH treatment for 2 h. The lysates of transfected cells were then applied to PPA. Total RNAs were isolated from heavy polysome fractions followed by performing 5'RACE to characterize the nucleotide sequences of truncated (D) exogenous *huORF^{chop}-luc* and (E) endogenous *huORF^{chop}-CHOP* transcripts. The first sequence at N-terminus of RNA samples from the truncated forms derived from exogenous *huORF^{chop}-luc* ($n = 14$) and endogenous *huORF^{chop}-CHOP* transcripts ($n = 11$) was determined; the percentages of positive colonies containing various 5' UTR lengths (truncated forms) of *luc* and *CHOP* transcripts among total colonies examined were calculated.

Source data are available online for this figure.

Truncated *huORF^{chop}-69-105-nt* transcript contains internal translation activity, but truncated *huORF^{chop}-81-105-nt* transcript does not

Luc and *CHOP* proteins could be produced from exogenous *huORF^{chop}-luc* and endogenous *huORF^{chop}-CHOP* mRNAs after Endouc binding and cleavage. Therefore, we hypothesized that the 5'-region of the truncated *huORF^{chop}* transcript may have internal

translational activity that enables the translation of DCS. The predicted RNA sequences of Endouc recognition, binding, and cleavage sites on the 105-nt *huORF^{chop}* RNA were located from 72 to 91 nts (Fig 7C). Thus, we first engineered a truncated form that only contains 69–105 nts RNA fragment (*huORF^{chop}-69-105-nt*), and then employed a pRF/phpRF bicistronic system (Terenin et al, 2017). In the pRF bicistronic reporter system, *Renilla luc* (Rluc) protein is translated in a cap-dependent manner from the first cistron through

ribosomal scanning, while Firefly luc (Fluc) protein is translated from the second cistron only if a fragment inserted at the upstream region possesses a cap-independent translation mechanism. Since the Fluc/Rluc ratio represents a cap-independent translation efficiency, four transcripts were designed to obtain Fluc/Rluc ratios. Appendix Fig S7A indicates the following: (i) *RF*: No insertion between *Rluc*- and *Fluc*-cistrons which served as mock control; (ii) *RF-huORF⁶⁹⁻¹⁰⁵* (*RF-huORF^{chop}-69-105-nt*; an experimental group); (iii) *RF-cmyc* (the 5'UTR of *c-myc* which served as positive control); and (iv) *RF-Non¹⁰⁵* (a 105-nt RNA encoding luc that served as negative control). Based on the value of Fluc/Rluc ratio, we determined the cap-independent translation efficiency of each inserted fragment. Following *in vitro* synthesis, these four bicistronic mRNAs were transfected individually into HEK293T cells, and their luc activities were determined by a dual-luc assay. The Fluc/Rluc ratio obtained from transfection of RNA transcribed from vector construct only with no insert (*RF*; mock group) was set as 1. Compared to the *RF* group, the Fluc/Rluc ratio from transfection of *RF-Non¹⁰⁵* transcript (negative control) did not increase (Appendix Fig S7A) suggesting that the 105-nt *luc* RNA did not contain internal translation activity. In contrast, the Fluc/Rluc ratio from transfection of *RF-cmyc* transcript (positive control) was dramatically increased ~100-fold compared to the *RF* group suggesting that the 5'UTR of *c-myc* contained strong internal translation activity consistent with the results reported by Stoneley *et al* (1998). Interestingly, the Fluc/Rluc ratio from transfection of the *RF-huORF⁶⁹⁻¹⁰⁵* transcript was increased 3.2-fold over that of control *RF* mRNA (Appendix Fig S7A) suggesting that the *RF-huORF⁶⁹⁻¹⁰⁵* RNA fragment also has internal translation activity.

The phpRF bicistronic reporter vector system excludes the possibility of either ribosomal reinitiation or read-through from the stop codon of the *Rluc* cistron to the start codon of the *Fluc* cistron. Thus, a stable palindromic sequence is inserted before the start codon of the first ORF of *Rluc* generating a stable mRNA hairpin (−55 Kcal/mol) that inhibits cap-dependent translation (Yang & Wang, 2019). Consequently, cap-dependent translation of the *Rluc* cistron is diminished, while cap-independent internal translation driven by downstream *Fluc* cistron is not affected. As depicted in Appendix Fig S7, four transcripts were designed as *hpRF* (mock control), *hpRF-huORF⁶⁹⁻¹⁰⁵* (an experimental group), *hpRF-cmyc* (positive control), and *hpRF-Non¹⁰⁵* (negative control). Since the amount of input mRNA was not significantly different (Appendix Fig S7A and C) and Rluc activity was no different among the four groups, the change in the Fluc/Rluc ratio was completely due to the change in the Fluc activity (Appendix Fig S7B and D).

As shown in Appendix Fig S7B, the Fluc/Rluc ratio from cells transfected with bicistronic mRNA containing *c-myc* (*hpRF-cmyc* transcript) was significantly increased: up to ~1,500-fold greater than the Fluc/Rluc ratio of *hpRF* mock control and *hpRF-Non¹⁰⁵* negative control groups. This increase indicates that the 5'UTR of *c-myc* contained pronounced internal translation activity. Interestingly, the Fluc/Rluc ratio of cells transfected with the *hpRF-huORF⁶⁹⁻¹⁰⁵* transcript was increased 80.5-fold over that of the *hpRF* mock control (Appendix Fig S7C). These findings strongly suggest that the *huORF^{chop}-69-105-nt* transcript has internal translation activity albeit relatively weaker than *c-myc*.

To further determine whether the truncated form of *huORF^{chop}-81-105-nt* derived from Endouc-cleaved *huORF^{chop}* also contains

internal translation activity, we engineered the 81-105-nt segment of *huORF^{chop}* where the cleavage site of Endouc was at 80G-81U. We then co-transfected *endouc* mRNA with bicistronic RNA fragment containing *huORF^{chop}-69-105-nt* and *huORF^{chop}-81-105-nt* into HEK293T cells. As shown in Appendix Fig S8, the Fluc/Rluc ratio in cells transfected with *endouc* mRNA was slightly increased from 3.4- to 5.5-fold in *RF-huORF⁶⁹⁻¹⁰⁵* mRNA (Appendix Fig S8A and B). The ratio was dramatically elevated from 43- to 226-fold in *hpRF-huORF⁶⁹⁻¹⁰⁵* mRNA compared to that of control *hpRF* mRNA (Appendix Fig S8C and D). Surprisingly, the internal translation activity driven by *huORF^{chop}-81-105-nt* was completely lost suggesting that the truncated Endouc-cut *huORF^{chop}* transcript from the T81 cleavage site to the end of the *huORF^{chop}* transcript (i.e., *huORF^{chop}-81-105-nt*) does not contain internal translation activity.

The internal translation activity possessed by *huORF^{chop}-69-105-nt* transcript is increased in the presence of Endouc

To investigate whether Endouc increases internal translation-dependent translation of the *huORF^{chop}* transcript, we co-transfected *endouc* mRNA combined with bicistronic RNA containing *huORF^{chop}-69-105-nt* transcript into HEK293T cells whereas co-transfection of *gfp* mRNA and *huORF^{chop}-69-105-nt* transcript served as a negative control. In the pRF bicistronic reporter system, overexpression of Endouc could increase the translation of DCS of *huORF^{chop}-69-105-nt* inserted in the intercistronic region (*RF-huORF⁶⁹⁻¹⁰⁵* transcript) because the Fluc/Rluc ratio was raised from 3.9 to 5.3 (Fig 9A). Moreover, overexpression of Endouc could dramatically increase the translation of the DCS reporter within *huORF^{chop}-69-105-nt* transcript (*hpRF-huORF⁶⁹⁻¹⁰⁵*) in the phpRF bicistronic reporter system in which a hairpin structure inhibits the cap-dependent translation (Rluc). This is because Fluc/Rluc ratio was elevated from 41- to 219-fold compared to that of *hpRF* control mRNA (Fig 9C). Again, the Rluc activity showed no difference among groups (Fig 9B and D) indicating that the change of Fluc/Rluc ratio was completely dependent on the change of Fluc activity. In contrast, if the 80G-81U site in the *huORF^{chop}-69-105-nt* transcript was mutated (*RF-huORF⁶⁹⁻¹⁰⁵-T81C/hpRF-huORF⁶⁹⁻¹⁰⁵-T81C*), then the internal translation activity was completely lost (Fig 9A and C). We conclude that (i) overexpressed Endouc increases the internal translation activity driven by *huORF^{chop}-69-105-nt* transcript and (ii) the 5'-region of uncapped truncated *huORF^{chop}-69-105-nt* may also contribute to continuous translation as mediated by internal translation initiation activity.

The *huORF^{chop}-69-105-nt* transcript possesses an IRES activity

We used the pRF/phpRF bicistronic system described above to demonstrate that the *huORF^{chop}-69-105-nt* transcript, but not the *huORF^{chop}-81-105-nt* transcript, contains internal translation activity. Next, we determined whether this *huORF^{chop}-69-105-nt* transcript possesses an IRES activity. To make this determination, we performed an *in vitro* system to transcribe polyA-tailed *Fluc* mRNA fused after *huORF^{chop}-69-105-nt* transcript which was capped with a normal m7Gppp (a 5'-capped form) or a non-functional ApppG (a 5' A-capped form) at the 5' end. However, the m7Gppp-capped mRNAs are translated in both a cap-dependent and a cap-independent manner, while A-capped mRNAs are only translated in a cap-independent manner. Therefore, to make the distinction between cap-dependence and cap-independence, we compared the translation

efficiency between m7Gppp- and A-capped mRNAs. To do this, we next used A-capped *myc* IRES transcripts fused at the upstream of a *Fluc* reporter to serve as a positive control. The A-capped 105 nt of luc cDNA (Non 105) served as a negative control. After a two-hr transfection of these transcripts in HEK293T cells, we found that the translation efficiency of A-capped *myc-Fluc* mRNA only reached approximately 15% of that driven by m7GpppG-capped *myc-Fluc* mRNA (Fig 10A). As expected, the reporter activity driven by A-capped *Fluc* mRNA (Fig 10B) and A-capped Non105 (Fig 10C) was very low (~1.5%). The A-capped full-length *huORF^{chop}-1-105-nt* reporter transcript (A-capped *huORF¹⁻¹⁰⁵Fluc*) exhibited only 1.5% of that driven by m7GpppG-capped *huORF¹⁻¹⁰⁵Fluc* (Fig 10D) suggesting that full-length *huORF^{chop}-1-105-nt* exhibited no IRES activity. We also found that the *huORF^{chop}-81-105-nt* transcript (A-capped *huORF⁸¹⁻¹⁰⁵Fluc*) showed no IRES activity (Fig 10F). Interestingly, the A-capped *huORF⁶⁹⁻¹⁰⁵Fluc* RNA fragment exhibited 4.3% reporter activity compared to m7GpppG-capped *huORF⁶⁹⁻¹⁰⁵Fluc* RNA (Fig 10E) suggesting that the uncapped *huORF^{chop}-69-105-nt* transcript does have IRES activity.

To further analyze whether the presence of Endouc impacts *huORF^{chop}-69-105-nt* IRES activity, we studied the luc activity of A-capped *huORF⁶⁹⁻¹⁰⁵Fluc* transcript in the presence of Endouc or Endouc^{K242A} in HEK293T cells. The results showed that the luc activity of A-capped monocistronic mRNAs containing full-length *huORF^{chop}* and *huORF^{chop}-69-105-nt* transcripts was induced in the presence of Endouc, but not in the presence of endoribonuclease-deficient mutant Endouc^{K242A} (Fig 10G) suggesting that *huORF^{chop}* IRES activity induced by Endouc is mediated through its endoribonuclease activity. Interestingly, the A-capped mRNA containing *huORF^{chop}-81-105-nt* failed to induce luc activity (Fig 10G) suggesting that the truncated uncapped *huORF^{chop}-81-105-nt* transcript generated from the cleavage of Endouc/ENDOU-1 on the full-length of *huORF^{chop}-1-105-nt* transcript at 80G-81U does not possess IRES activity unlike the *huORF^{chop}-69-105-nt* transcript.

To further analyze whether the presence of Endouc impacts the *huORF^{chop}-69-105-nt* IRES activity, we studied the luc activity of ApppG-capped *huORF⁶⁹⁻¹⁰⁵Luc* transcript in the presence of Endouc or Endouc^{K242A} in HEK293T cells. The results showed that the luc activity of ApppG-capped monocistronic mRNAs containing full-length *huORF^{chop}* and *huORF^{chop}-69-105-nt* transcripts was induced in the presence of Endouc but not in the presence of endoribonuclease-deficient mutant Endouc^{K242A} (Fig 10G) suggesting that the *huORF^{chop}* IRES activity induced by Endouc is mediated through its endoribonuclease activity. Interestingly, the ApppG-capped mRNA containing *huORF^{chop}-81-105-nt* transcript failed to induce luc activity (Fig 10G). Additionally, in the absence of Endouc, only *huORF⁶⁹⁻¹⁰⁵*, but not full-length *huORF^{chop}*, displayed weak IRES activity (Fig 10G). Strikingly, however, when Endouc was overexpressed in cells, both *huORF^{chop}-69-105-nt* and full-length *huORF^{chop}* transcripts displayed IRES activity (Fig 10G).

Following the logic of this line of collective evidence, we suggest that an inhibitory element could be present in *huORF^{chop}-1-68-nt* causing the repression of IRES activity. In clear contrast, when Endouc is overexpressed in cells, the inhibitory structure of *huORF^{chop}* transcript is disrupted via endoribonuclease, likely altering the inhibitory element presented in *huORF^{chop}-1-68-nt* but promoting the IRES activity driven by *huORF^{chop}-69-105-nt* to then facilitate the translation of *CHOP* DCS.

Discussion

In this study, we found an RNA-binding endoribonuclease Endouc/ENDOU-1 protein involved in mediating *CHOP* translation through suppression of the inhibitory *huORF^{chop}* transcript during ER stress. We made several discoveries during the course of our investigation. (i) Endouc/ENDOU-1 is a stress-responsive protein that can rapidly increase in the presence of such stressors as heat-shock and hypoxia. (ii) Endouc/ENDOU-1 induces *huORF^{chop}-tag* reporter and *CHOP* translation in an endoribonuclease-dependent manner. (iii) While the level of p-eIF2 α is increased during *CHOP* translation, *CHOP* induced by Endouc/ENDOU-1 is independent of p-eIF2 α since Endouc/ENDOU-1 alone causes *CHOP* to be partially translated. (iv) However, Endouc/ENDOU-1 and p-eIF2 α are under the control of a feedback loop that enforces cooperativity in the translation of *CHOP* DCS within *huORF^{chop}* transcript to reach a maximal level. (v) Endouc/ENDOU-1 can directly bind the *huORF^{chop}* transcript and cleave it at the 80G-81U site. (vi) Overexpression of Endouc promotes the shifting of *huORF^{chop}-tagged* transcripts from monosome fractions toward polysome fractions. (vii) Unlike the *huORF^{chop}-81-105-nt* transcript, the truncated uncapped *huORF^{chop}-69-105-nt* transcript possesses an IRES activity. We began our investigation by questioning the involvement of regulatory proteins in suppressing *huORF^{chop}-TI*. Based on the results above, we determined that Endouc/ENDOU-1 plays a distinctly positive role in post-transcriptional regulation of the human *CHOP* gene.

Within the *huORF^{chop}-69-105-nt* transcript, the core sequence (72–91 nts) that contains the Endouc recognition site is highly conserved among different species (Young *et al*, 2016). However, the polypeptide encoded by *huORF^{chop}* RNA, especially the carboxyl-terminal portion, is important for forming the inhibitory function of *huORF^{chop}* (Jousse *et al*, 2001; Palam *et al*, 2011). Young *et al* (2016) proposed that an IFI sequence at amino acid 28–30 encoded by the 81–90 nts of *huORF^{chop}* transcript causes ribosomes to stall at the upstream sequence of AUG, which, in turn, prevents translation of the DCS. Unexpectedly, however, they found that this ribosomal stall mediated by the IFI sequence is not regulated in a stress-dependent manner. Thus, the mechanism that allows stalled ribosomes to reinitiate translation at the DCS of *huORF^{chop}* transcript during ER stress is still unclear.

Nevertheless, our study explains how Endouc/ENDOU-1 participates in post-translational control mediated by *huORF^{chop}* transcript, and we propose a simple potential mechanistic model to illustrate the role of Endouc/ENDOU-1 in *huORF^{chop}*-mediated translational control (Fig 11). The 72–91 nts within the full-length of *huORF^{chop}-1-105-nt* transcript in which the IFI sequence and 80G-81U are included constitute an important segment required for *huORF^{chop}* transcript to form a unique hairpin structure. We learned that an inhibitory conformation occurs and that ribosomes stall at 81–90 nts of *huORF^{chop}* transcript (Young *et al*, 2016) when cells are in the normal condition. Thus, the translation of DCS within the *huORF^{chop}* transcript is blocked by the *huORF^{chop}-TI* due to the low levels of Endouc/ENDOU-1 and p-eIF2 α . However, Endouc/ENDOU-1 is quickly induced when cells encounter stress, bind directly to the hairpin structure of *huORF^{chop}* transcript formed by its 72–91-nt sequences, and cleave it at the 80G-81U site. This process blocks *huORF^{chop}-TI* by the conformational change of the inhibitory *huORF^{chop}*

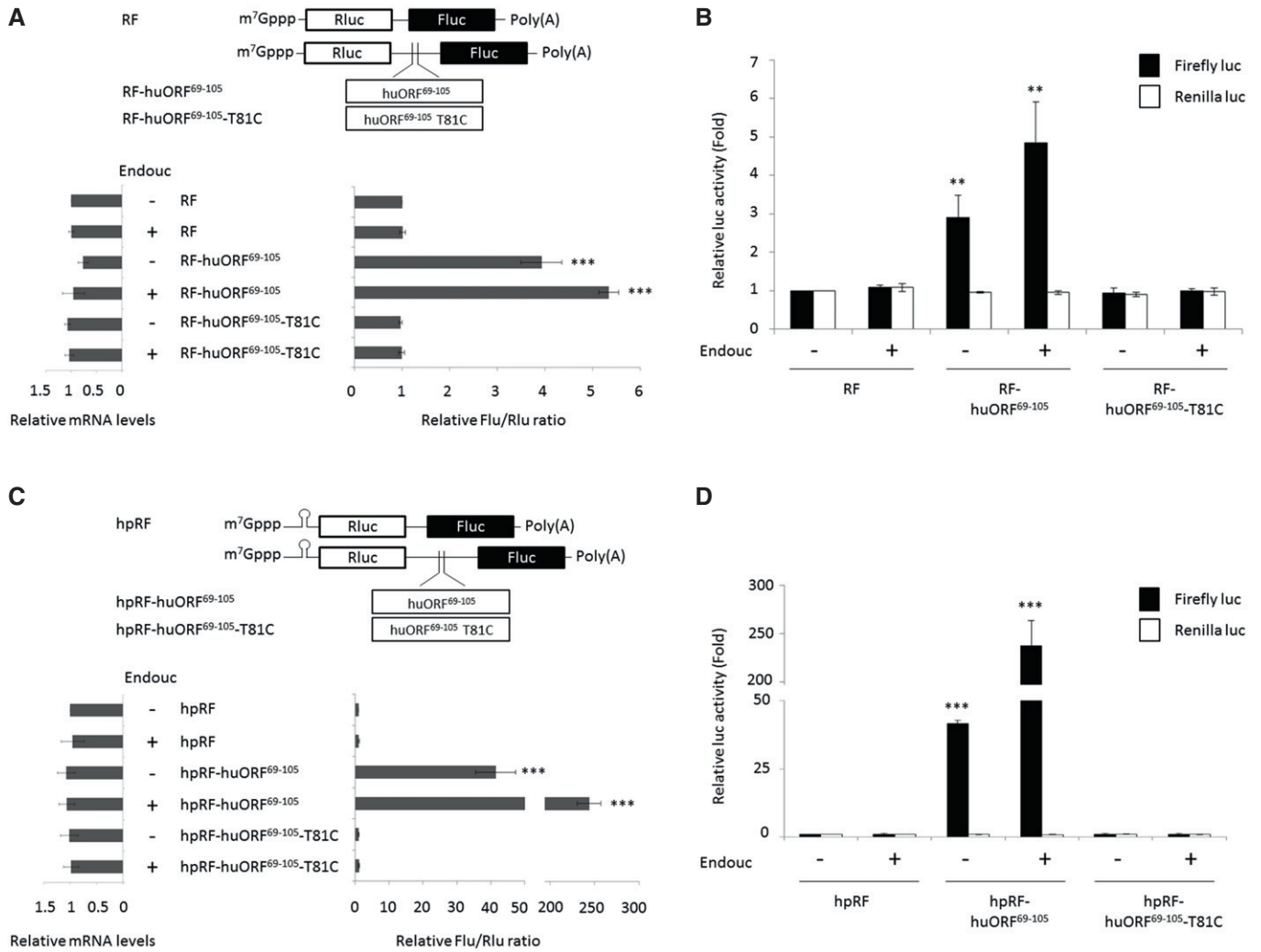


Figure 9. The 5' region of the cleaved *huORF^{chop}* transcript contains internal translation activity.

A Schematic representation of RF bicistronic transcript is shown above the bar graphs. Rluc: *Renilla luciferase* (blank box); Fluc: *Firefly luciferase* (solid box). The luc activity of HEK293T cells transfected with bicistronic mRNA, as indicated, in the presence (+) or absence (–) of *endouc-Flag* mRNA was determined. The relative luc activity of transfected cells shown on the right was normalized by the amount of the transfected bicistronic transcript shown on the left. The relative luc activity was represented by the fold increase of Fluc/Rluc ratio over that obtained from control group, normalized as 1. The luc activity was measured by dual-luciferase assay, and its corresponding bicistronic mRNAs were measured by RT–qPCR. The values were calculated from three independent experiments and presented as mean ± SD (*n* = 3). Student's *t*-test was used to determine significant differences between each group (***) (*P* < 0.001).

B The luc activity of Fluc (solid column) versus Rluc (blank column) in HEK293T cells transfected with bicistronic mRNAs shown in A was presented as an increase in fold over that obtained from control group of RF which was normalized as 1. These data suggested that the change of Fluc/Rluc ratio shown in A was entirely dependent on the change of Fluc activity. The data were averaged from three independent experiments and presented as mean ± SD (*n* = 3). Student's *t*-test was used to determine significant differences between each group (***P* < 0.005).

C Schematic representation of hpRF bicistronic transcript. Rluc: *Renilla luciferase* (blank box); Fluc: *Firefly luciferase* (solid box). The luc activity of HEK293T cells transfected with bicistronic mRNA, as indicated, in the presence (+) or absence (–) of *endouc-Flag* mRNA was determined. The relative luc activity of transfected cells shown on the right was normalized by the amount of the transfected bicistronic transcript shown on the left. The relative luc activity was represented by the fold increase of Fluc/Rluc ratio over that obtained from control group, normalized as 1. The luc activity was measured by dual-luciferase assay, and its corresponding bicistronic mRNAs were measured by RT–qPCR. The values were calculated from three independent experiments and presented as mean ± SD (*n* = 3). Student's *t*-test was used to determine significant differences between each group (***) (*P* < 0.001).

D The luc activity of Fluc (solid column) versus Rluc (blank column) in HEK293T cells transfected with bicistronic mRNAs shown in C was presented as an increase in fold over that obtained from control group of hpRF which was normalized as 1. These data suggested that the change of Fluc/Rluc ratio shown in C was entirely dependent on the change of Fluc activity. The data were averaged from three independent experiments and presented as mean ± SD (*n* = 3). Student's *t*-test was used to determine significant differences between each group (***) (*P* < 0.001).

structure, in turn, releasing the stalled ribosomes to scan through the *huORF^{chop}* transcript and reinitiate at AUG of the main DCS within *huORF^{chop}* transcript. This activity constitutes

continuous translation of *CHOP* mRNA via IRES activity driven by the truncated uncapped form of *huORF^{chop}*-69-105-nt and by the increase of p-eIF2 α induced by Endouc/ENDOU-1.

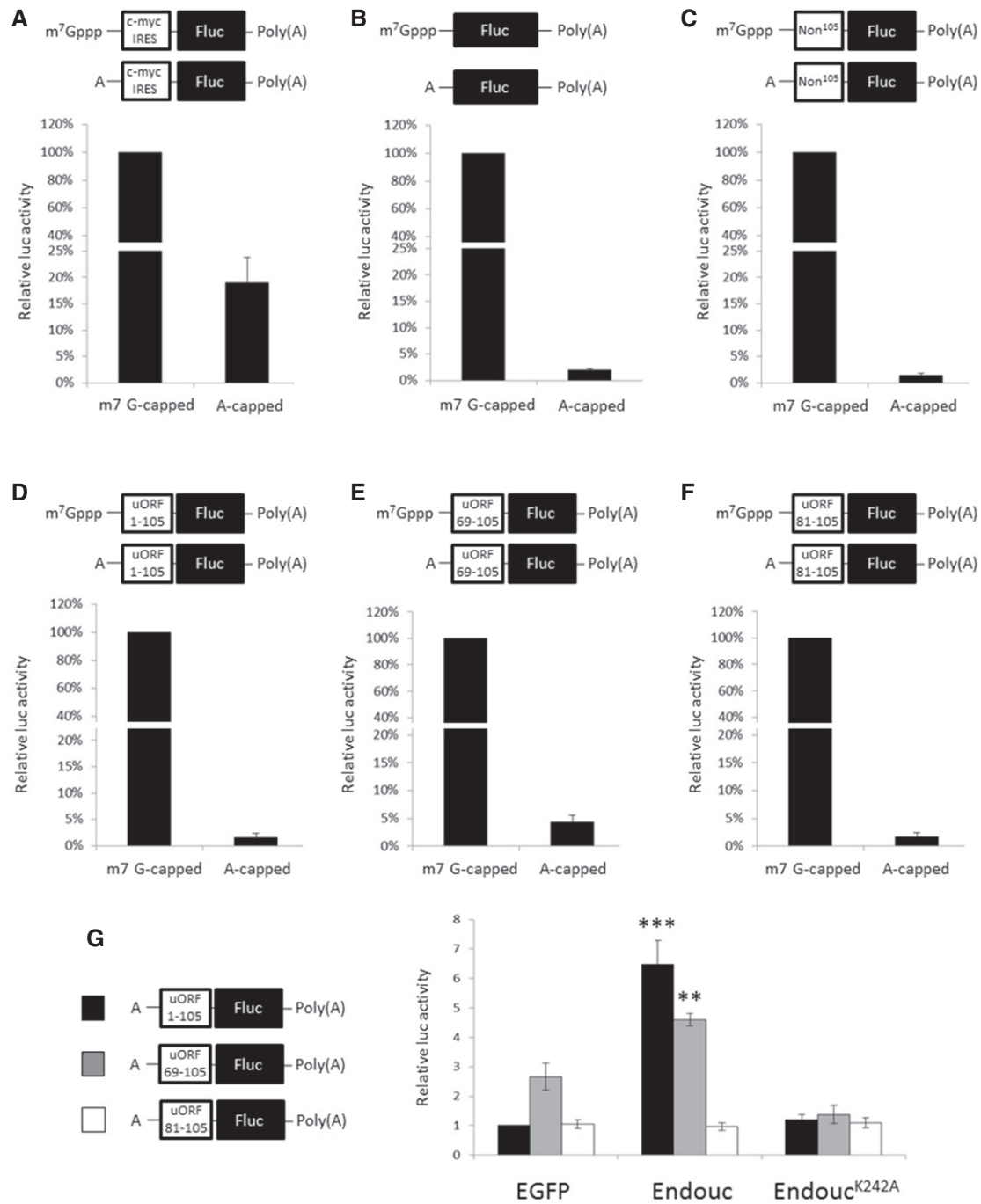


Figure 10. Comparison between cap-dependent and IRES-dependent translation of the *huORF^{chop}* transcript containing reporter.

A–F Schematic representation of capped (m7G-capped) and A-capped (non-functional capped) monocistronic mRNAs with poly(A)-tail-encoded firefly luciferase (Fluc) and fused upstream with (A) c-myc IRES, (B) no insertion, (C) non-specific 105-nt luc RNA (Non¹⁰⁵), (D) *huORF^{chop}*-1-105-nt, (E) *huORF^{chop}*-69-105-nt, and (F) *huORF^{chop}*-81-105-nt as shown above each bar graph. The RNA transfection assay of each transcript equipped with m7G-capped or A-capped monocistronic mRNA in HEK293T cells was compared. To normalize the luc activities of capped and A-capped *Fluc* transcripts, the m7G-capped *Renilla luc* (Rluc) mRNA was used as an internal control. The luc activity of cells transfected with cap-monocistronic mRNA in each graph was set as 100%.

G The luc activity driven by the indicated A-capped monocistronic mRNA in the presence of Endouc or Endouc^{K242A} in HEK293T cells. The m7G-capped *Rluc* mRNA was used as an internal control to normalize the activities of A-cap *Fluc* transcripts. The *egfp* mRNA was used as a negative control, and the luc activity of cells transfected with *egfp* mRNA and A-cap *Fluc* mRNA containing full-length *huORF^{chop}*-1-105-nt was set to 1. The data were averaged from three independent experiments and presented as mean ± SD (n = 3). Student's t-test was used to determine significant differences between each group (**P < 0.005, ***P < 0.001).

Using the pRF/phpRF bicistronic system, we demonstrated that the *huORF^{chop}*-69-105-nt transcript, but not the *huORF^{chop}*-81-105-nt transcript, contains internal translation activity. Furthermore, by comparing the translation efficiency between m7Gppp- and A-capped mRNAs, we also demonstrated that the uncapped truncated *huORF^{chop}*-69-105-nt transcript possesses an IRES activity. It is known that RNA structure determines the function of IRES elements (Martinez-Salas et al., 2018), and thus, the RNA structure of *huORF^{chop}*-69-105-nt may recruit ribosomes and initiation factors for DCS translation. Meanwhile, polysomal profiling analysis demonstrated that Endouc/ENDOU-1 associates with ribosomal proteins in translational fractions suggesting that Endouc/ENDOU-1 also plays a role in recruiting other factors that are necessary for DCS translation processes. On the other hand, we found that the *huORF^{chop}*-69-105-nt, but not full-length *huORF^{chop}*, displayed weak IRES activity in the absence of Endouc/ENDOU-1. However, both *huORF^{chop}*-69-105-nt and full-length *huORF^{chop}* transcripts displayed an IRES activity in Endouc/ENDOU-1-overexpressed cells (Fig 10G) suggesting an inhibitory function of *huORF^{chop}*-1-68-nt able to repress the IRES activity driven by *huORF^{chop}*-69-105-nt.

Therefore, we propose that the cleavage of Endouc/ENDOU-1 on the *huORF^{chop}* transcript accomplishes the following tasks: (i) disrupt the inhibitory structure formed by the 72-91-nt sequence of *huORF^{chop}* transcript, (ii) facilitate RNA conformational changes to alter the inhibitory element of *huORF^{chop}*-1-68-nt, and (iii) strengthen the IRES activity driven by *huORF^{chop}*-69-105-nt. When 80G-81U sequences were mutated, the translation of DCS was not enhanced by the increase of Endouc/ENDOU-1. This observation strengthens our hypothesis that the disruption of inhibitory conformation by the binding and cleavage of Endouc/ENDOU-1 is required to reinitiate the translation of the *CHOP* gene under stress conditions. While beyond the scope of the present paper, additional factors involved in the interaction among Endouc/ENDOU-1, *huORF^{chop}*-1-68-nt, and *huORF^{chop}*-69-105-nt transcripts are worthy of further investigation.

The translation initiation factor eIF2 can mitigate cellular injury or, alternatively, can induce apoptosis when cells encounter environmental stresses. During stress, the alpha subunit of eIF2 at S51 can be phosphorylated by a number of related protein kinases. Phosphorylation of eIF2 reduces global translation allowing cells to conserve resources and initiate a reconfiguration of gene expression to effectively manage stress. On the other hand, eIF2 phosphorylation can also induce the translation of specific mRNAs such as *ATF4* and *CHOP* (Harding et al, 2000; Lu et al, 2004; Vattem & Wek, 2004; Palam et al, 2011). Palam et al (2011), proposed that enhanced p-eIF2 during stress facilitates ribosomal bypass of inhibitory *huORF^{chop}* elements for continued DCS translation. These results suggest that the increase of p-eIF2 α as mediated by Endouc/ENDOU-1 can promote a cooperativity required to overcome the inhibitory *huORF^{chop}* element under stress.

The results demonstrated that both Endouc and p-eIF2 α are required for *CHOP* translation; however, p-eIF2 α is not the only protein able to facilitate *CHOP* translation to reach its maximal level during stress. This conclusion is supported by other researchers. For example, the level of *CHOP* remained low when Dey et al (2010) used UV irradiation to elicit p-eIF2 α expression. Similarly, Ghosh et al (2011) reported that the absence of Sirtuin1 in cells resulted in

the elevated and prolonged phosphorylation of eIF2 α but reduced and delayed the induction of the downstream *CHOP* protein. Moreover, cells treated with Salubrinal—a drug which acts as a specific inhibitor of eIF2 α phosphatase enzymes and prevents dephosphorylation of eIF2 α during stress condition—led to an increase of p-eIF2 α expression but caused a decrease in *CHOP* expression (Luo et al, 2003; Oyadomari & Mori, 2004; Duan et al, 2014). Tyagi et al (2015) reported that a ubiquitous small GTPase, Rheb, could enhance p-eIF2 α and increase ATF4 level. However, their downstream *CHOP* was not affected. Collectively, this line of evidence leads to the conclusion that trans-acting factors other than p-eIF2 α might be involved in suppressing the inhibitory effect of *huORF^{chop}* elements under stress. Indeed, this research was undertaken to identify putative proteins other than known ribosomal proteins such as eIF2 α that might be directly involved in suppressing *huORF^{chop}*-TI under stress.

Accordingly, after performing microarray analysis of cells between suppressing and non-suppressing *huORF^{chop}* elements under stress in an *in vivo* system, we identified an RNA-binding protein, Endouc/ENDOU-1, that appears to play a key role in facilitating *CHOP* translation through the suppression of *huORF^{chop}*-TI under stress stimuli. Overexpression of Endouc/ENDOU-1 can induce eIF2 α phosphorylation through the PKR pathway. PKR is a double-stranded RNA (dsRNA)-dependent protein kinase that plays multiple roles in response to different stress situations such as virus infection (Dabo & Meurs, 2012). The interaction between PKR and dsRNA is independent of any specific RNA nucleotide motif or sequences (Minks et al, 1979). Moreover, about 30–80 nt of dsRNA is enough to activate PKR activity (Manche et al, 1992; Nanduri et al, 1998). Thus, we speculate that the Endouc-cleaved *huORF^{chop}* transcript may form a dsRNA that contributes to PKR activation, but, again, further elucidation of this topic is outside the scope of this work yet worthy of further investigation.

Many stress factors contain a uORF cassette on their 5'UTR to control translation in response to environmental stresses (Hinnebusch, 2014). ATF4 is one of the key stress factors, and its mRNA contains a uORF cassette on the 5'UTR (Harding et al, 2000). Although we did not examine the translational effects of Endouc on *huORF^{ATF4}* using luciferase assay, Western blot analysis showed that the protein level of ATF4 did not change when cells overexpressed either Endouc or ENDOU-1 suggesting that Endouc does not specifically interact with *huORF^{ATF4}* (Fig EV4D).

Meantime, the stress factor GADD34 also contains an inhibitory uORF sequence and could be induced by Endouc/ENDOU-1 (Fig EV4D). However, the increase of GADD34 protein is indirectly controlled by Endouc/ENDOU-1 because the translation of GADD34 is p-eIF2 α -dependent, and p-eIF2 α can be partially induced by Endouc/ENDOU-1. Therefore, although the transcripts of *CHOP*, *GADD34*, and *ATF4* contain inhibitory uORF segments to mediate the translation of DCS during stress, the regulatory mechanisms among these three genes are quite distinct. Our data demonstrate that Endouc/ENDOU-1 is selective for the uORF segment of the human *chop* transcript rather than the uORF segments of other genes. We propose that this might result from the unique hairpin structure of *huORF^{chop}* formed by its 71–91-nt sequence that enables Endouc/ENDOU-1 to specifically interact with and cleave *huORF^{chop}* transcript thus repressing the translation inhibition mediated by *huORF^{chop}*. However, it is very possible that Endouc might be

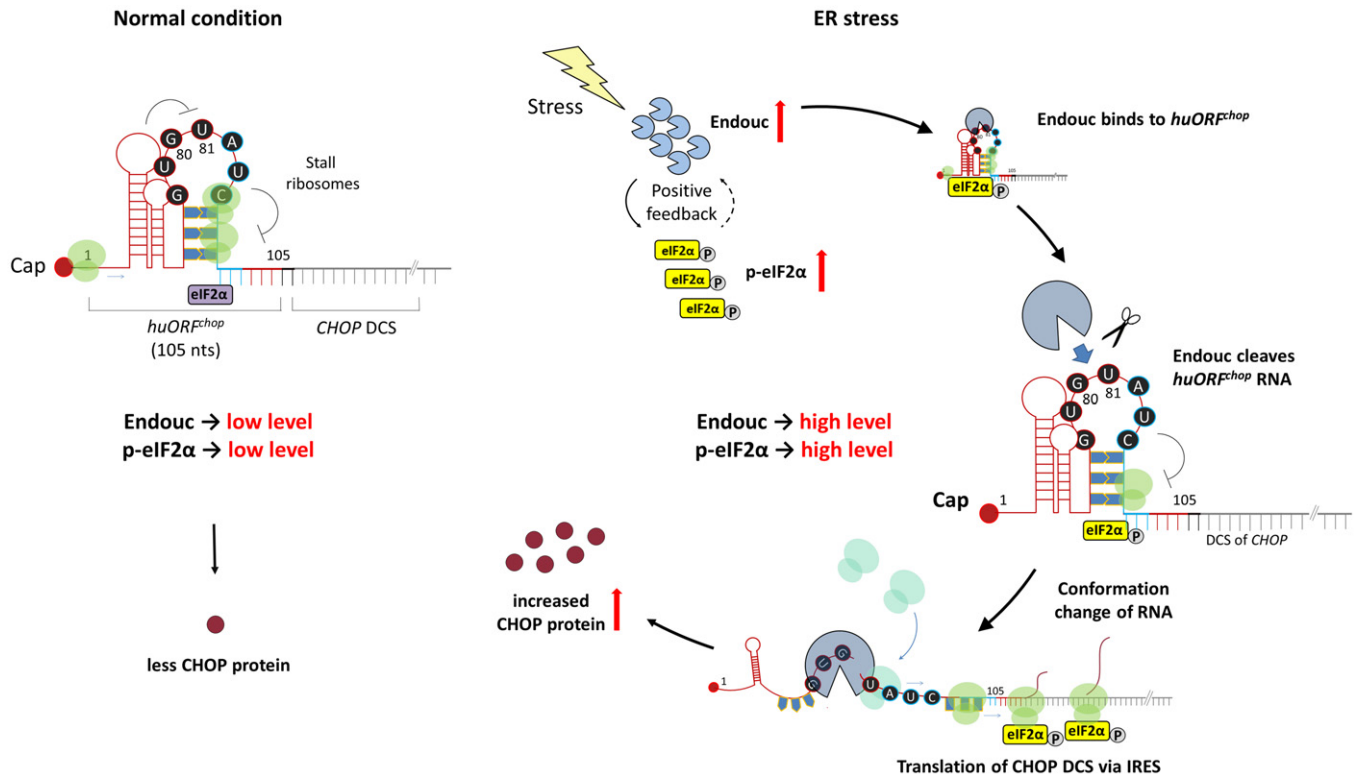


Figure 11. Schematic representation illustrating how Endouc/ENDOU acts as a positive modulator of human *CHOP* mRNA translation by suppressing the inhibitory *huORF^{chop}* transcript.

During normal conditions, the translation of *CHOP* protein is blocked by *huORF^{chop}*-TI due to ribosomes stalled at 81–90 nts within the 105-nt *huORF^{chop}* transcript. However, Endouc/ENDOU is quickly produced when cells encounter environmental stress, e.g., heat-shock and hypoxia as in the present work. It binds to the hairpin structure of *huORF^{chop}* transcript formed at 72–91 nts and cleaves it at the 80G–81U site. This endonuclease activity changes the conformation of inhibitory structure formed by *huORF^{chop}* transcript, in turn, releasing the stalled ribosomes to scan through the *huORF^{chop}* transcript and reinitiate at AUG of the main downstream coding sequence (DCS) of *huORF^{chop}* transcript. Finally, *CHOP* transcript is continuously translated via the IRES activity driven by *huORF^{chop}*–69–105-nt and the increase of p-eIF2 α induced by Endouc/ENDOU.

specific for other targets as well. This will also be the subject of further study.

Materials and Methods

Zebrafish husbandry, transgenic line, and signal observation

Zebrafish AB strain and transgenic line were cultured as previously described (Westerfield, 2000; Lee *et al.*, 2014). Transgenic line *huORFZ* harbors a DNA fragment containing the *huORF^{chop}* element fused with the downstream GFP cDNA (*huORF^{chop}-gfp*) and driven by a cytomegalovirus promoter (Lee *et al.*, 2011). The translation of transgenic *huORF^{chop}-gfp* mRNA is absolutely inhibited by *huORF^{chop}* element in *huORFZ* embryos during normal condition. However, the downstream GFP translated from *huORF^{chop}-gfp* mRNA is exclusively apparent in the CNS of heat-shock- and hypoxia-treated *huORFZ* embryos (Lee *et al.*, 2011, 2014; Zeng *et al.*, 2016). Specifically, a subtype cell population, which responds with high sensitivity to ER stress, exists in the CNS and, as a result, exhibits a GFP signal. Therefore, the *huORFZ* line is a good *in vivo* system with which to study the molecular mechanism of uORF-

mediated translational control. Fluorescence was visualized with a fluorescent stereomicroscope (Leica) and a confocal spectral microscope (Leica). The experiments and treatments of this zebrafish model have been reviewed and approved by the National Taiwan University and Mackay Medical College Institutional Animal Care and Use Committee with ethics approval number NTU-102-EL-24 and A1050012, respectively.

RNA extraction, cDNA synthesis, microinjection, and WISH

Total RNAs were extracted from about 50–100 embryos using 500 μ l of TRIzol Reagent (Lee *et al.*, 2011). The cDNA pools were generated by Superscript III Reverse Transcriptase Kit (Invitrogen). Microinjection and WISH were performed as previously described (Lee *et al.*, 2011) with the exception of *endouc* which was labeled by Digoxigenin (DIG) and used as a probe with anti-DIG antibody (Roche; 1:8,000).

Conditions of heat-shock and hypoxic stresses

Since heat-shock and hypoxia could cause *huORFZ* embryos to express strong GFP signals in CNS tissues (Lee *et al.*, 2011), we

submitted fish to these two treatments to collect GFP(+) and GFP(−) cells individually. For heat-shock treatment, we followed the protocol described by Lee *et al* (2011). Briefly, a 2 ml centrifuge tube filled with 30 dechorionated zebrafish embryos from transgenic line *huORFZ* at 72 hpf was subjected to 40°C for 1 h. Then, the treated embryos were collected into a 3-cm Petri dish and incubated at 28.5°C until they developed at 96 hpf. Treatment to induce hypoxia followed the protocol described by Zeng *et al* (2016). Briefly, a deoxygenated solution was prepared as 80 ml of EM (pH 5.8) and placed in a 100-ml serum bottle capped with a rubber stopper having a glass tube. It was kept at 28°C for 10 min, followed by pumping 99% nitrogen for 5 min at the gas flow rate of 10–20 l/min. The oxygen concentration in deoxygenated solution is less than 0.5 ppm. A 15 ml centrifuge tube filled with 100 dechorionated *huORFZ* embryos at 72 hpf was treated with the deoxygenated solution for 2 h at 28°C. After treatment, embryos were collected into a 9-cm Petri dish and incubated at 28°C until they developed at 96 hpf. These treated 96-hpf embryos were ready for further experiments.

Cell capture and microarray

To study the genes involved in *huORF^{chop}-TI*, zebrafish embryos at 72 hpf were separately treated with hypoxia and heat-shock, followed by examining GFP signals during 96 hpf. After sections were performed in brain, we employed Laser microdissection (Leica LMD 7000) to separately capture the GFP(+) and GFP(−) cells from the same subtype. Equal numbers of GFP(+) and GFP(−) cells were centrifuged and resuspended in 200 µl of TRIzol Reagent (Invitrogen). Total RNAs were extracted using the RNeasy Plus Micro kit (Qiagen), and the expression levels of genes between GFP(+) and GFP(−) cells were analyzed by Welgene Biotech Co. (Taiwan). The Zebrafish Oligo Microarray kit (Agilent, Taiwan) was used to perform color microarray from the two noted stresses. Output from Agilent's feature extraction software was imported using GeneSpring GX 7.3.1 software (Agilent Technologies). The ratios of treatment and reference raw intensity data were log-transformed and normalized using locally weighted least squares regression (Lowess regression) normalization. All these candidates were subcloned, expression patterns were examined, and expression levels were compared between heat-shocked and WT embryos using WISH.

RT-qPCR analysis

Samples were added to 50–100 µl of TRIzol reagent (Invitrogen) and stored at −80°C. Total RNAs were isolated according to the manufacturer's instructions. The qPCR was analyzed by Seeding Biotech Co. (Taiwan). The first-strand cDNA was generated using 1 mg of total RNA. Both cDNA concentrations were adjusted to 200 ng/ml, and RT-qPCR was performed using the 7900HT Fast Real-Time PCR System (Applied Biosystems, USA) according to the manufacturer's instructions. Forward and reverse primers designed for cloning each gene by PCR are presented in Appendix Table S3. Detection of spliced *xbp1* and *CHOP* mRNAs followed the procedure described previously (van Schadewijk *et al*, 2012; B'chir *et al*, 2013). For *CHOP* mRNA stability assay, HEK293T cells were cultured in the presence or absence of TH for 3 h, followed by actinomycin D (10 µg/ml) treatment for 0, 1, 2, and 3 h. After total

RNAs were extracted, *CHOP* mRNA was then quantified by RT-qPCR and normalized to 18S rRNA expression. To compare the stability of full-length *CHOP* transcript and cleaved *CHOP* mRNA, MEF cells were transfected with plasmid pCS2-Endouc-Flag for 24 h, followed by actinomycin D (10 µg/ml) treatment for 0, 1, 2, and 3 h. After total RNAs were extracted, an adaptor linked at the 5' end was added for cDNA synthesis as described in the SMARTer RACE 5'/3' kit (Takara). Then, we designed specific primers containing adaptor-linked target sequence which could specifically anneal to either full-length *CHOP* or cleaved *CHOP* cDNA for the RT-qPCR experiment. Primers are listed in Appendix Table S3. The data were normalized by the expression level of 18S rRNA.

Cell culture, transfection, and drug treatment

Cell lines HEK293T, HeLa, and U373MG were cultured and transfected as previously described (Chen *et al*, 2010). Insect cells Sf21 were cultured and transfected as described by Fu *et al* (2012). The MEF WT and eIF2 α ^{S51A} (S51A) mutant cells were cultured following the protocol described by Scheuner *et al* (2001). Briefly, MEF WT and S51A cells were maintained in DMEM high glucose (Gibco) plus 10% fetal bovine serum (Gibco); 1% penicillin/streptomycin (Gibco); 1% non-essential amino acid (Sigma); and 1% sodium pyruvate (Sigma). For RNA transfection assay, HEK293T cells were transfected in a 24-well plate using Lipofectamine 3000 according to the manufacturer's instruction (Invitrogen). We transfected 300 ng of capped or A-capped monocistronic Firefly reporter and 10 ng of capped *Renilla* RNAs (as a transfection control) in each well. Transfection of 300 ng capped bicistronic mRNA and 50 ng of *egfp* mRNA served as negative control. Relative luc activity was measured at 2 h post-transfection. For drug treatment, cultures were replaced by fresh medium, incubated for 2 h, and the following chemicals individually added: Dimethyl sulfoxide (DMSO; Sigma) served as the control group, 1 µM TH served as an ER stress inducer, and 200 nM ISRIB served as an inhibitor of integrated stress response (Sidrauski *et al*, 2015). Cells were then harvested after treatment for 1–8 h as indicated.

Knockdown by small interfering RNA (siRNA) in cell lines

All siRNAs were designed and synthesized by Qiagen. AllStars Negative Control siRNA (Qiagen) was used to validate non-silencing siRNA.

Dual-luciferase assay

Dual-luciferase assay performed on cells (Chen *et al*, 2010) and zebrafish embryos (Lin *et al*, 2013) was previously described, except 5 ng/µl of pHRG-TK (internal control) and puORF^{chop}-luc reporter construct were used. For each experiment in zebrafish, embryos at 96 hpf were collected and divided into three groups to carry out *in vivo* dual-luciferase assay ($n = 60$), RT-qPCR ($n = 50$), and Western blot analysis ($n = 90$).

Western blotting and immunostaining

Western blot analysis and immunostaining followed the procedures described previously (Lin *et al*, 2013), except that the following

antibodies were used: eIF2 α (1:1,000; CST); p-eIF2 α (1:1,000; CST); zebrafish eIF2 α (1:500; GeneTex); zebrafish DDIT3 (1:500; Techom); PERK (1:1,000; CST); p-PERK (1:1,000; Abcam); Bip (1:1,000; CST); p58IPK (1:1,000; CST); Flag (1:30,000; Abcam); ENDOU-1 (1:1,000; Abcam); GADD34 (1:1,000; ABD Serotec); ATF4 (1:1,000; Abcam); PKR (1:1,000; SC); human pPKR (1:1,000; Abcam); mouse pPKR (1:1,000; Sigma-Aldrich); GAPDH (1:10,000; Abcam); and α -tubulin (1:5,000; Sigma). Fifty μ g protein extracts were loaded in each lane to detect the protein level. Ninety μ g of extracts were loaded to analyze the specific proteins from zebrafish embryos.

Northern blotting, RNase activity assay, RNA-binding assay, and RNA synthesis

Northern blot analysis was performed as previously described (Hsu et al, 2010; Rio, 2014), except huORF-5' antisense and huORF-3' antisense were synthesized (Mdbio Bioscience, Taiwan) and labeled with radioisotope p³² to serve as probes. The probes to detect zebrafish 18S RNA and human GAPDH RNA served as internal controls and were PCR-amplified using primers listed in Appendix Table S3. For the RNase activity assay, a concentration of 10 μ g purified recombinant Endouc was mixed with cell extracts (10 μ g) in 10- μ l reaction buffer (50 mM NaCl, 25 mM HEPES, pH 7.4, 1 mM DTT, 0.1% glycerol, and 20 U RNasin), in which 5 pmole of biotin-labeled RNA was contained. Samples were incubated at 37°C for 30–60 min, and RNAs were electrophoresed on 10–15% polyacrylamide gel containing 8 M Urea. For RNA-binding assay, biotin-labeled RNA substrate was generated using the Pierce RNA 3' End Biotinylation kit (Thermo). Recombinant Endouc was incubated with RNA substrate for 30 min at 37°C. The results were analyzed on 7 and 15% polyacrylamide gel containing 8 M urea and stained with the Chemiluminescent Nucleic Acid Detection Module kit (Thermo). Biotin-labeled nucleic acid probes were detected using the Chemiluminescent Nucleic Acid Detection Module Kit (Thermo). For biotin-labeled RNA synthesis, full-length *huORF^{chop}* RNA (105 nt) was synthesized using the T7 Transcription kit (Thermo). Two pmole of template was used, and reaction was 5 h. Then, these small RNAs were labeled with biotin using the Pierce RNA 3' End Biotinylation kit (Thermo). Primers T7 + huORF (Full)-F plus T7 + huORF(Full)-R, T7 + huORF-M (Full)-F plus T7 + huORF-M (Full)-R, and T7 + luc 1-105 fragment-F plus luc 1-105 fragment-R were used to amplify full-length *huORF^{chop}*, mutant *huORF^{chop}*, and the luc 105 bp DNA fragment, respectively. The biotin-labeled *huORF^{chop}* template DNA was synthesized by Mdbio Bioscience. To synthesize mRNAs used for cell transfection, we generated capped transcripts using mMessage mMachine T7 Ultra kits (Ambion), precipitated with LiCl in 10 mM Tris-HCl (pH 8.5) buffer, and, finally, examined on agarose gel electrophoresis.

Plasmid construction

The *huORF^{chop}* fragment and plasmid pcDNA-GFP (pGFP) were described previously (Lee et al, 2011). The cDNAs encoding zebrafish Endouc and three human ENDOU isoforms were cloned by RT-PCR from the cDNA pools to generate pCS2-zEndouc, pCS2-hENDO-1, pCS2-hENDO-2 and pCS2-hENDO-3. Zebrafish Endouc contains a signal peptide at N-terminus and a XendoU

domain (amino acid residues 131–285), which is highly conserved among eukaryotes (Lee et al, 2017). To analyze Endouc domain mapping, the constructs of Endouc Δ^{1-25} (1–25 single peptide deletion), Endouc Δ^{26-136} (26–136 domain deletion), Endouc $\Delta^{137-298}$ (137–298 domain deletion), and Endouc $\Delta^{299-310}$ (C-terminal domain deletion) were generated by PCR. Above PCR products were individually subcloned into pCS2 + to generate pCS2-zEndouc Δ^{1-25} , pCS2-zEndouc Δ^{26-136} , pCS2-zEndouc $\Delta^{137-298}$, and pCS2-zEndouc $\Delta^{299-310}$. The ORFs of *endouc*, *endouc $\Delta^{137-298}$* , *endouc $\Delta^{299-310}$* , *endouc^{K242A}*, and *ENDO-1* fused with FLAG peptide were engineered to construct pCS2-Endouc-Flag, pCS2-Endouc $\Delta^{137-298}$ -Flag, pCS2-Endouc $\Delta^{299-310}$ -Flag, pCS2-Endouc^{K242A}-Flag, and pCS2-ENDOU-1-Flag, respectively. The C-terminus of Endouc fused with FLAG was cut by *PstI* and *XhoI* and inserted into the plasmids containing zebrafish *endouc* variant to generate pCS2-Endouc Δ^{1-25} -Flag, pCS2-Endouc Δ^{26-136} -Flag and pCS2-Endouc^{H181A}-Flag. The C-terminal domain of ENDOU-1 fused with FLAG was cut by *NcoI* and *NotI* and inserted into plasmids containing human ENDOU isoforms to generate pCS2-ENDOU-2-Flag and pCS2-ENDOU-3-Flag, while it was cut by *EcoRV* and *NotI* and inserted into pCS2-ENDOU-1^{H285A} to generate pCS2-ENDOU-1^{H285A}-Flag. To analyze the endoribonuclease activity of Endouc/ENDO-1, we previously compared the amino acid sequence between human ENDOU isoforms, zebrafish Endouc, and *Xenopus* XendoU (Lee et al, 2017). E243, H244, E249, H259, and K302 are necessary for human ENDOU-2 endoribonuclease activity (Laneve et al, 2008), while H162 and K224 are necessary for *Xenopus* XendoU RNase activity, corresponding to H244 and K302 of human ENDOU-2, respectively (Schwarz & Blower, 2014). Zebrafish Endouc was therefore mutated at H181 (Endouc^{H181A}) and K242 (Endouc^{K242A}) to alanine, corresponding to H244 and K302 of human ENDOU-2, respectively. H285 in human ENDOU-1, corresponding to H244 in human ENDOU-2, was also mutated to alanine. These point-mutated codons responsible for endonuclease activity were obtained by PCR site-directed mutagenesis to generate pCS2-zEndouc^{K242A}, pCS2-zEndouc^{H181A}, and pCS2-hENDO-1^{H285A}. Plasmid p3XFlag-eIF2 α ^{S51A} and p3XFlag-eIF2 α ^{S51A} were obtained by PCR site-directed mutagenesis from p3XFlag-eIF2 α .

The pRF/phpRF bicistronic assay system

The DNA fragments encoding 81 to 105 nts of *huORF^{chop}* transcript (*huORF⁸¹⁻¹⁰⁵*), 69–105 nts of *huORF^{chop}* cassette (*huORF⁶⁹⁻¹⁰⁵*), and its mutant *huORF⁶⁹⁻¹⁰⁵*-T81C were obtained by primer annealing, which contained a complete hairpin structure, as we predicted, using Predict a Secondary Structure Web Server (Fig 7C), and inserted between the cDNAs encoding *Rluc* and *Fluc* in a dual-reporter system of pRF and phpRF (Stoneley et al, 1998; Jopling & Willis, 2001) to generate plasmids pRF-uORF⁶⁹⁻¹⁰⁵, pRF-uORF⁸¹⁻¹⁰⁵, pRF-uORF⁶⁹⁻¹⁰⁵-T81C, and phpRF-uORF⁶⁹⁻¹⁰⁵, phpRF-uORF⁸¹⁻¹⁰⁵, and phpRF-uORF⁶⁹⁻¹⁰⁵-T81C, respectively. A 105-bp DNA fragment obtained by PCR from *Renilla* gene of pRL was inserted into pRF and phpRF to generate pRF-Non¹⁰⁵ and phpRF-Non¹⁰⁵ (negative controls), respectively. Primers used to construct these plasmids are shown in Appendix Table S3. Above plasmids were linearized with *BamHI*. The capped and polyA-tailed bicistronic transcripts were synthesized with the T7 RiboMAX large-scale RNA production system (Promega) according to the manufacturer's protocol. All the bicistronic mRNAs *in vitro* transcribed from the desired plasmid

constructs were transfected into HEK293T cells for 2 h, followed by analysis of luc activity. The luc activity was measured by dual-luciferase assay, and its corresponding bicistronic mRNAs were measured by RT-qPCR. The relative luc activity, normalized by the relative mRNA level, was represented by the increase in fold of Fluc/Rluc ratio over that obtained from control group.

Purification of recombinant Endouc

The DNA fragment encoding recombinant Endouc-Flag was inserted into the Baculovirus recombinant transfer vector pVL1392 (BD) to generate pVL1392-Endouc-Flag, which was transfected into insect cell line Sf21 to produce recombinant Endouc-Flag. This Endouc-Flag protein was purified by anti-Flag beads (Sigma).

Bioinformatics

To predict the RNA secondary structure of *huORF^{chop}* motif, we used <http://rna.urmc.rochester.edu/RNAstructureWeb/index.html>

Polysome profile analysis

The use of sucrose gradient centrifugation to perform polysome profiling was described previously (Chen *et al*, 2010), except that cells were incubated with Cycloheximide (100 µg/ml) for 5 min at 37°C, and the fractionated RNA (500 ng) was subjected to RT-PCR. Primers are listed in Appendix Table S3.

5'RACE

After monosomal and polysomal RNAs were fractionated, we isolated the RNA samples to analyze the 5'-end sequences of all truncated forms derived from *huORF^{chop}* transcript. The cDNA synthesis and 5'RACE followed the protocols described in the SMARTer RACE 5'/3' kit (Takara). The specific primers used for 5'RACE are listed in Appendix Table S3. The conditions of PCR amplification were (i) for uORF-luc fragment: 94°C 30 s, 72°C 30 s (5 cycles), 94°C 30 s, 70°C 30 s, 72°C 25 s (5 cycles), 94°C 30 s, 68°C 30 s, 72°C 25 s (for 25 cycles); and (ii) for uORF-CHOP fragment: 94°C 30 s, 72°C 30 s (5 cycles), 94°C 30 s, 70°C 30 s, 72°C 30 s (5 cycles), 94°C 30 s, 68°C 30 s, and 72°C 30 s. After PCR amplification, the RACE products were characterized by electrophoresis and subcloned using the In-Fusion HD cloning kit (Takara). Finally, the candidate RACE products were sequenced using M13F primers.

Statistical analysis

Data were obtained by the average value from three independent experiments and presented as mean ± SD. Difference levels were analyzed using Student's *t*-test.

Data availability

This study includes no data deposited in external repositories.

Expanded View for this article is available online.

Acknowledgements

This work was supported by the National Science Council, Taiwan (109-2313-B-715-002, 109-2313-B-715-003), partially supported by Mackay Medical College, Taiwan (1091B12, 1081B12, and 1051B19), and partially supported by Liver Disease Prevention and Treatment Research Foundation, Taiwan. We are very grateful for the support of Mr. Spencer Lee and Dr. Hsiao-Ching Nien, the Liver Disease Prevention and Treatment Research Foundation, Taipei, Taiwan. The MEF cell line was provided and shipped by Dr. Sung Hoon Back (University of Ulsan, ROK) with permission of Prof. R. J. Kaufman (Sanford Burnham Prebys Medical Discovery Institute, USA). We thank Prof. Sheng-Chung Lee, IBC, NTU, for helpful discussion, and Dr. Shih-Tong Jeng and Dr. Yung-Shu Kuan for helping with the isotope experiment. We also thank Technology Commons, CLS, NTU, for helping with the LMD and confocal microscopy. We are grateful to Prof. Anne E. Willis (MRC Toxicology Unit, University of Cambridge, UK) for providing plasmids pRF, phpRF, pRF-c-myc, and phpRF-c-myc; Dr. Yi-Ling Lin (Institute of Biomedical Sciences, Academia Sinica, Taiwan) for providing plasmid pcDNA3-PKRΔ6; and Dr. Jin-Won Cho (Yonsei University, ROK) for providing plasmid p3XFlag-eIF2α.

Author contributions

H-CL and C-YF conducted the main experiments. C-YL, J-RH, and T-YH prepared plasmids, proteins, cell lines, and transgenic fish. H-CL performed LMD and microarray. K-YL and T-YH performed the polysome profile assay. H-YT and J-RH performed RNA structure prediction. J-CS and H-JT conceptualized and directed the project. H-JT edited the draft written by H-CL and C-YF.

Conflict of interest

The authors declare that they have no conflict of interest.

References

- von Arnim AG, Jia Q, Vaughn JN (2014) Regulation of plant translation by upstream open reading frames. *Plant Sci* 214: 1–12
- B'chir W, Maurin AC, Carraro V, Averous J, Jousse C, Muranishi Y, Parry L, Stepien G, Fafournoux P, Bruhat A (2013) The eIF2α/ATF4 pathway is essential for stress-induced autophagy gene expression. *Nucleic Acids Res* 41: 7683–7699
- Barbosa C, Peixeiro I, Romão L (2013) Gene expression regulation by upstream open reading frames and human disease. *PLoS Genet* 9: e1003529
- Barbosa C, Romão L (2014) Translation of the human erythropoietin transcript is regulated by an upstream open reading frame in response to hypoxia. *RNA* 20: 594–608
- Barone MV, Crozat A, Tabae A, Philipson L, Ron D (1994) CHOP (GADD153) and its oncogenic variant, TLS-CHOP, have opposing effects on the induction of G1/S arrest. *Genes Dev* 8: 453–464
- Bhardwaj K, Liu P, Leibowitz JL, Kao CC (2012) The coronavirus endoribonuclease Nsp15 interacts with retinoblastoma tumor suppressor protein. *J Virol* 86: 4294–4304
- Bhardwaj K, Sun J, Holzenburg A, Guarino LA, Kao CC (2006) RNA recognition and cleavage by the SARS coronavirus endoribonuclease. *J Mol Biol* 361: 243–256
- Caffarelli E, Maggi L, Fatica A, Jiricny J, Bozzoni I (1997) A novel Mn⁺⁺-dependent ribonuclease that functions in U16 SnRNA processing in *X. laevis*. *Biochem Biophys Res Commun* 233: 514–517
- Calvo SE, Pagliarini DJ, Mootha VK (2009) Upstream open reading frames cause widespread reduction of protein expression and are polymorphic among humans. *Proc Natl Acad Sci USA* 106: 7507–7512

- Chen YJ, Tan BC, Cheng YY, Chen JS, Lee SC (2010) Differential regulation of CHOP translation by phosphorylated eIF4E under stress conditions. *Nucleic Acids Res* 38: 764–777
- Chew GL, Pauli A, Rinn JL, Regev A, Schier AF, Valen E (2013) Ribosome profiling reveals resemblance between long non-coding RNAs and 5' leaders of coding RNAs. *Development* 140: 2828–2834
- Chew GL, Pauli A, Schier AF (2016) Conservation of uORF repressiveness and sequence features in mouse, human and zebrafish. *Nat Commun* 7: 11663
- Col B, Oltean S, Banerjee R (2007) Translational regulation of human methionine synthase by upstream open reading frames. *Biochim Biophys Acta* 1769: 532–540
- Dabo S, Meurs EF (2012) dsRNA-dependent protein kinase PKR and its role in stress, signaling and HCV infection. *Viruses* 4: 2598–2635
- Dey S, Baird TD, Zhou D, Palam LR, Spandau DF, Wek RC (2010) Both transcriptional regulation and translational control of ATF4 are central to the integrated stress response. *J Biol Chem* 285: 33165–33174
- Duan Z, Zhao J, Fan X, Tang C, Liang L, Nie X, Liu J, Wu Q, Xu G (2014) The PERK-eIF2 α signaling pathway is involved in TCDD-induced ER stress in PC12 cells. *Neurotoxicology* 44: 149–159
- Ebina I, Takemoto-Tsutsumi M, Watanabe S, Koyama H, Endo Y, Kimata K, Igarashi T, Murakami K, Kudo R, Ohsumi A et al (2015) Identification of novel Arabidopsis thaliana upstream open reading frames that control expression of the main coding sequences in a peptide sequence-dependent manner. *Nucleic Acids Res* 43: 1562–1576
- Fu CY, Su YF, Lee MH, Chang GD, Tsai HJ (2012) Zebrafish Dkk3a protein regulates the activity of *myf5* promoter through interaction with membrane receptor integrin $\alpha 6b$. *J Biol Chem* 287: 40031–40042
- Ghosh HS, Reizis B, Robbins PD (2011) SIRT1 associates with eIF2- α and regulates the cellular stress response. *Sci Rep* 1: 150
- Gioia U, Laneve P, Dlakic M, Arceci M, Bozzoni I, Caffarelli E (2005) Functional characterization of XendoU, the endoribonuclease involved in small nucleolar RNA biosynthesis. *J Biol Chem* 280: 18996–19002
- Harding HP, Novoa I, Zhang Y, Zeng H, Wek R, Schapira M, Ron D (2000) Regulated translation initiation controls stress-induced gene expression in mammalian cells. *Mol Cell* 6: 1099–1108
- He F, Li X, Spatrick P, Casillo R, Dong S, Jacobson A (2003) Genome-wide analysis of mRNAs regulated by the nonsense-mediated and 5' to 3' mRNA decay pathways in yeast. *Mol Cell* 12: 1439–1452
- Hinnebusch AG (2014) The scanning mechanism of eukaryotic translation initiation. *Annu Rev Biochem* 83: 779–812
- Hsu RJ, Lin CY, Hoi HS, Zheng SK, Lin CC, Tsai HJ (2010) Novel intronic microRNA represses zebrafish *myf5* promoter activity through silencing dickkopf-3 gene. *Nucleic Acids Res* 38: 4384–4393
- Iacono M, Mignone F, Pesole G (2005) uAUG and uORFs in human and rodent 5'untranslated mRNAs. *Gene* 349: 97–105
- Inaba N, Ishige H, Ijichi M, Satoh N, Ohkawa R, Sekiya S, Shirotake S, Takamizawa H, Renk T, Bohn H (1982) Immunohistochemical detection of pregnancy-specific protein (SP1) and placenta-specific tissue proteins (PP5, PP10, PP11 and PP12) in ovarian adenocarcinomas. *Oncodev Biol Med* 3: 379–389
- Jopling CL, Willis AE (2001) N-myc translation is initiated via an internal ribosome entry segment that displays enhanced activity in neuronal cells. *Oncogene* 20: 2664–2670
- Jousse C, Bruhat A, Carraro V, Urano F, Ferrara M, Ron D, Fournoux P (2001) Inhibition of CHOP translation by a peptide encoded by an open reading frame localized in the chop 5'UTR. *Nucleic Acids Res* 29: 4341–2001
- Kindler E, Gil-Cruz C, Spanier J, Li Y, Wilhelm J, Rabouw HH, Züst R, Hwang M, Vokovski P, Stalder H et al (2017) Early endonuclease-mediated evasion of RNA sensing ensures efficient coronavirus replication. *PLoS Pathog* 13: e1006195
- Koromilas AE, Roy S, Barber GN, Katze MG, Sonenberg N (1992) Malignant transformation by a mutant of the IFN-inducible dsRNA-dependent protein kinase. *Science* 257: 1685–1689
- Kozak M (1987) An analysis of 5'-noncoding sequences from 699 vertebrate messenger RNAs. *Nucleic Acids Res* 15: 8125–8148
- Laneve P, Altieri F, Fiori ME, Scaloni A, Bozzoni I, Caffarelli E (2003) Purification, cloning, and characterization of XendoU, a novel endoribonuclease involved in processing of intron-encoded small nucleolar RNAs in *Xenopus laevis*. *J Biol Chem* 278: 13026–13032
- Laneve P, Gioia U, Ragno R, Altieri F, Di Franco C, Santini T, Arceci M, Bozzoni I, Caffarelli E (2008) The tumor marker human placental protein 11 is an endoribonuclease. *J Biol Chem* 283: 34712–34719
- Lee HC, Chen YJ, Liu YW, Lin KY, Chen SW, Lin CY, Lu YC, Hsu PC, Lee SC, Tsai HJ (2011) Transgenic zebrafish model to study translational control mediated by upstream open reading frame of human chop gene. *Nucleic Acids Res* 39: e139
- Lee HC, Fu CY, Zeng CW, Tsai HJ (2017) Embryonic expression patterns of Eukaryotic EndoU ribonuclease family gene *endouc* in zebrafish. *Gene Expr Patterns* 25–26: 66–70
- Lee HC, Lu PN, Huang HL, Chu C, Li HP, Tsai HJ (2014) Zebrafish transgenic line *huORFZ* is an effective living bioindicator for detecting environmental toxicants. *PLoS One* 9: e90160
- Lin CY, Lee HC, Fu CY, Ding YY, Chen JS, Lee MH, Huang WJ, Tsai HJ (2013) MiR-1 and miR-206 target different genes to have opposing roles during angiogenesis in zebrafish embryos. *Nat Commun* 4: 2829
- Lu PD, Harding HP, Ron D (2004) Translation re-initiation at alternative open reading frames regulates gene expression in an integrated stress response. *J Cell Biol* 167: 27–33
- Luo S, Baumeister P, Yang S, Abcouwer SF, Lee AS (2003) Induction of Grp78/BiP by translational block: Activation of the Grp78 promoter by ATF4 through an upstream ATF/CRE site independent of the endoplasmic reticulum stress elements. *J Biol Chem* 278: 37375–37385
- Manche L, Green SR, Schmedt C, Mathews MB (1992) Interactions between double-stranded RNA regulators and the protein kinase DAI. *Mol Cell Biol* 12: 5238–5248
- Matsui M, Yachie N, Okada Y, Saito R, Tomita M (2007) Bioinformatic analysis of post-transcriptional regulation by uORF in human and mouse. *FEBS Lett* 581: 4184–4188
- Mendell JT, Sharifi NA, Meyers JL, Martinez-Murillo F, Dietz HC (2004) Nonsense surveillance regulates expression of diverse classes of mammalian transcripts and mutes genomic noise. *Nat Genet* 36: 1073–1078
- Minks MA, West DK, Benveniste S, Baglioni C (1979) Structural requirements of double-stranded RNA for the activation of 2',5'-oligo(A) polymerase and protein kinase of interferon-treated HeLa cells. *J Biol Chem* 254: 10180–10183
- Nanduri S, Carpick BW, Yang Y, Williams BR, Qin J (1998) Structure of the double-stranded RNA-binding domain of the protein kinase PKR reveals the molecular basis of its dsRNA-mediated activation. *EMBO J* 17: 5458–5465
- Novoa I, Zhang Y, Zeng H, Jungreis R, Harding HP, Ron D (2003) Stress-induced gene expression requires programmed recovery from translational repression. *EMBO J* 22: 1180–1187
- Oyadomari S, Mori M (2004) Roles of CHOP/GADD153 in endoplasmic reticulum stress. *Cell Death Differ* 11: 381–389
- Palam LR, Baird TD, Wek RC (2011) Phosphorylation of eIF2 facilitates ribosomal bypass of an inhibitory upstream ORF to enhance CHOP translation. *J Biol Chem* 286: 10939–10949

- Park JS, Luethy JD, Wang MG, Fargnoli J, Fornace Jr AJ, McBride OW, Holbrook NJ (1992) Isolation, characterization and chromosomal localization of the human GADD153 gene. *Gene* 116: 259–267
- Poe JC, Kountikov EI, Lykken JM, Natarajan A, Marchuk DA, Tedder TF (2014) EndoU is a novel regulator of AICD during peripheral B cell selection. *J Exp Med* 211: 57–69
- Pooggin MM, Futterer J, Skryabin KG, Hohn T (2001) Ribosome shunt is essential for infectivity of cauliflower mosaic virus. *Proc Natl Acad Sci USA* 98: 886–891
- Raghavan A, Ogilvie RL, Reilly C, Abelson ML, Raghavan S, Vasdevani J, Krathwohl M, Bohjanen PR (2002) Genome-wide analysis of mRNA decay in resting and activated primary human T lymphocytes. *Nucleic Acids Res* 30: 5529–5538
- Ramani AK, Nelson AC, Kapranov P, Bell I, Gingeras TR, Fraser AG (2009) High resolution transcriptome maps for wild-type and nonsense-mediated decay-defective *Caenorhabditis elegans*. *Genome Biol* 10: R101
- Renzi F, Panetta G, Vallone B, Brunori M, Arcenci M, Bozzoni I, Laneve P, Caffarelli E (2006) Large-scale purification and crystallization of the endoribonuclease XendoU: troubleshooting with His-tagged proteins. *Acta Crystallogr Sect F Struct Biol Cryst Commun* 62: 298–301
- Ricagno S, Egloff MP, Ulferts R, Coutard B, Nurizzo D, Campanacci V, Cambillau C, Ziebuhr J, Canard B (2006) Crystal structure and mechanistic determinants of SARS coronavirus nonstructural protein 15 define an endoribonuclease family. *Proc Natl Acad Sci USA* 103: 11892–11897
- Rio DC (2014) Northern blots for small RNAs and microRNAs. *Cold Spring Harb Protoc* 2014: 793–797
- Roberts LO, Jopling CL, Jackson RJ, Willis AE (2009) Viral strategies to subvert the mammalian translation machinery. *Prog Mol Biol Transl Sci* 90: 313–367
- Romano PR, Green SR, Barber GN, Mathews MB, Hinnebusch AG (1995) Structural requirements for double-stranded RNA binding, dimerization, and activation of the human eIF-2 α kinase DAI in *Saccharomyces cerevisiae*. *Mol Cell Biol* 15: 365–378
- Rutkowski DT, Arnold SM, Miller CN, Wu J, Li J, Gunnison KM, Mori K, Sadighi Akha AA, Raden D, Kaufman RJ (2006) Adaptation to ER stress is mediated by differential stabilities of pro-survival and pro-apoptotic mRNAs and proteins. *PLoS Biol* 4: e374
- Sachs MS, Geballe AP (2006) Downstream control of upstream open reading frames. *Genes Dev* 20: 915–921
- Scheuner D, Song B, McEwen E, Liu C, Laybutt R, Gillespie P, Saunders T, Bonner-Weir S, Kaufman RJ (2001) Translational control is required for the unfolded protein response and in vivo glucose homeostasis. *Mol Cell* 7: 1165–1176
- Schwarz DS, Blower MD (2014) The calcium-dependent ribonuclease XendoU promotes ER network formation through local RNA degradation. *J Cell Biol* 207: 41–57
- Sharova LV, Sharov AA, Nedorezov T, Piao Y, Shaik N, Ko MS (2009) Database for mRNA half-life of 19 977 genes obtained by DNA microarray analysis of pluripotent and differentiating mouse embryonic stem cells. *DNA Res* 16: 45–58
- Sidrauski C, McGeachy AM, Ingolia NT, Walter P (2015) The small molecule ISRIB reverses the effects of eIF2 α phosphorylation on translation and stress granule assembly. *Elife* 4: e05033
- Snijder EJ, Bredenbeek PJ, Dobbe JC, Thiel V, Ziebuhr J, Poon LL, Guan Y, Rozanov M, Spaan WJ, Gorbalenya AE (2003) Unique and conserved features of genome and proteome of SARS-coronavirus, an early split-off from the coronavirus group 2 lineage. *J Mol Biol* 331: 991–1004
- Stoneley M, Paulin FE, Le Quesne JP, Chappell SA, Willis AE (1998) C-Myc 5' untranslated region contains an internal ribosome entry segment. *Oncogene* 16: 423–428
- Terenin IM, Smirnova VV, Andreev DE, Dmitriev SE, Shatsky IN (2017) A researcher's guide to the galaxy of IRESs. *Cell Mol Life Sci* 74: 1431–1455
- Tu YC, Yu CY, Liang JJ, Lin E, Liao CL, Lin YL (2012) Blocking double-stranded RNA-activated protein kinase PKR by Japanese encephalitis virus nonstructural protein 2A. *J Virol* 86: 10347–10358
- Tyagi R, Shahani N, Gorgen L, Ferretti M, Pryor W, Chen PY, Swarnkar S, Worley PF, Karbstein K, Snyder SH et al (2015) Rheb inhibits protein synthesis by activating the PERK-eIF2 α signaling cascade. *Cell Rep* 10: 684–693
- Ujisawa T, Ohta A, Ii T, Minakuchi Y, Toyoda A, Ii M, Kuhara A (2018) Endoribonuclease ENDU-2 regulates multiple traits including cold tolerance via cell autonomous and nonautonomous controls in *Caenorhabditis elegans*. *Proc Natl Acad Sci USA* 115: 8823–8828
- van Schadewijk A, van't Wout EFA, Stolk J, Hiemstra PS (2012) A quantitative method for detection of spliced X-box binding protein-1 (XBP1) mRNA as a measure of endoplasmic reticulum (ER) stress. *Cell Stress Chaperones* 17: 275–279
- Vattem KM, Wek RC (2004) Reinitiation involving upstream ORFs regulates ATF4 mRNA translation in mammalian cells. *Proc Natl Acad Sci USA* 101: 11269–11274
- Westerfield M (2000) *The Zebrafish Book. A Guide for the Laboratory Use of Zebrafish (Danio rerio)*. Eugene, OR: University of Oregon Press
- Yaman I, Fernandez J, Liu H, Caprara M, Komar AA, Koromilas AE, Zhou L, Snider MD, Scheuner D, Kaufman RJ et al (2003) The zipper model of translational control: a small upstream ORF is the switch that controls structural remodeling of an mRNA leader. *Cell* 113: 519–531
- Yang Y, Wang Z (2019) IRES-mediated cap-independent translation, a path leading to hidden proteome. *J Mol Cell Biol* 11: 911–919
- Young SK, Palam LR, Wu C, Sachs MS, Wek RC (2016) Ribosome elongation stall directs gene-specific translation in the integrated stress response. *J Biol Chem* 291: 6546–6558
- Young SK, Wek RC (2016) Upstream open reading frames differentially regulate gene-specific translation in the integrated stress response. *J Biol Chem* 291: 16927–16935
- Zeng CW, Kamei Y, Wang CT, Tsai HJ (2016) Subtypes of hypoxia-responsive cells differentiate into neurons in spinal cord of zebrafish embryos after hypoxic stress. *Biol Cell* 108: 357–377
- Zhou D, Palam LR, Jiang L, Narasimhan J, Staschke KA, Wek RC (2008) Phosphorylation of eIF2 directs ATF5 translational control in response to diverse stress conditions. *J Biol Chem* 283: 7064–7073
- Zhou J, Wan J, Shu XE, Mao Y, Liu XM, Yuan X, Zhang X, Hess ME, Brüning JC, Qian SB (2018) N⁶-Methyladenosine guides mRNA alternative translation during integrated stress response. *Mol Cell* 69: 636–647



License: This is an open access article under the terms of the Creative Commons Attribution-NonCommercial-NoDeriv 4.0 License, which permits use and distribution in any medium, provided the original work is properly cited, the use is non-commercial and no modifications or adaptations are made.